

Dynamic Exception Points for Fair Liver Allocation

Mustafa Akan¹ · Musa Celdir · Sridhar Tayur

Tepper School of Business, Carnegie Mellon University

akan@andrew.cmu.edu, erenceldir@gmail.com, stayur@cmu.edu

Problem Definition: There are disparities in access to livers based on transplant patients' height - which disproportionately affects women across ethnicities, in addition to Hispanics and Asians broadly - because they can receive transplants from a smaller pool of available deceased donors for medical reasons. Reduced likelihood of transplantation leads to higher mortality rates and longer waiting times. Remedying this unfairness is a top priority for United Network for Organ Sharing (UNOS), the policy-making entity in the US.

Academic/Practical Relevance: We analyze fairness within the current US liver allocation system where patients on the waiting list receive priority dynamically, based on their Model for End-Stage Liver Disease (MELD) scores, which reflect the severity of liver disease. We propose a simple adjustment - providing additional (exception) points based on height and MELD score - that can be easily implemented in practice, which materially reduces the disparity without sacrificing overall efficiency.

Methodology: We model the liver allocation system as a multiclass fluid model of overloaded queues with multiple heterogeneous servers, which captures the disease evolution by allowing the patients to switch between classes over time, e.g., patients waiting for transplantation may get sicker/better, or may die. We impose explicit equity constraints for all static patient classes, i.e., height. We characterize the optimal solution to the fluid model under the objective of minimizing pre-transplant mortality using the duality framework for optimal control problems. The discretized version of the optimal policy is numerically solved using estimates from clinical data and a detailed simulation study demonstrates its effectiveness.

Results: We show that the optimal policy, called the Equity Adjusted Mortality Risk Policy, is an intuitive dynamic index policy, where the indices depend on patients' acceptance probabilities of the organ offers, mortality risks, and the shadow prices calculated from the dual dynamical system. This optimal policy advocates ranking patients based on their short-term mortality risk adjusted for equity among static (i.e., height) classes. The shadow prices of the equity constraints in the optimal control problem are novel in the organ transplant context, as is, even more importantly, their interpretation as MELD exception points, since they can be seamlessly mapped into the system already in practice. Providing these exception points to shorter patients dynamically increases their chances of receiving a transplant. Our simulations show that for women, the disparity can be almost completely eliminated. Hispanics and Asians greatly benefit from receiving these MELD exception points as well. These improved fairness can be achieved without decreasing the overall efficiency of the current liver allocation system.

¹This research is supported by grant CMMI-1334194 from NSF and the Marc Onetto Faculty Fellowship in Operations.

Managerial Implications: Our work provides a remedy to reduce the disparities in access to liver transplantation within the MELD-based allocation that is currently unfair to women and Hispanics/Asians.

Keywords: Fairness, Equity, Liver Allocation Policy, Organ Transplantation, MELD Exception Score

1 Introduction

Liver transplantation is the only viable treatment for End-Stage Liver Disease (ESLD) and acute liver failure. Causes of ESLD include viral hepatitis, cirrhosis, non-alcoholic fatty liver disease, and hepatocellular carcinoma (HCC); it is the 12th leading cause of death in the United States (Cox-North et al. 2013). Patients with ESLD and acute liver failure join the transplant waiting list managed by the United Network for Organ Sharing System (UNOS) because the number of patients exceeds the number of organs available for transplantation. As of October 16, 2023, 10,166 patients were waiting for a liver transplant in the United States; 13,019 patients joined the liver transplant waiting list, but only 9,701 livers were donated in 2020 (UNOS 2021). Due to the shortage of organ supply, the median waiting time until receiving a liver transplant is more than three years for an adult and more than 40,000 patients died while waiting for a liver transplant during 1995-2020 (UNOS 2021).

Given the severity of ESLD and the long waiting times of patients until receiving a liver transplant, fairness of the allocation of a limited supply of organs becomes an important issue to be addressed by policy makers. In their three general principles of organ allocation, UNOS (2010) places fairness along with efficiency and respect for patients' autonomy in making their decisions of accepting/rejecting organs. Within this context, we observe from the historical data that there are disparities in access to transplantation based on patients' blood type, height, and gender. Data from the University of California San Francisco (UCSF) Liver Center, see Table 1, show that shorter patients have a lower probability of receiving a liver transplant. Because women have a smaller stature statistically, the disparity due to height also causes disproportionately long waiting times for women.

These disparities in organ access are due to the fact that shorter patients can receive liver transplants from a smaller pool of available organs due to organ size incompatibility. Implantation of a large liver in a small recipient brings surgical difficulties (Reddy et al. 2013), and the unmatched metabolic demand of the recipient, as well as the physiologic mismatch, aggravates the damage to the liver graft, inevitably leading to graft failure (Kyota and Seigo 2016). The pool of adult donor livers has relatively few small livers nationally because most deceased-donor livers come from men; therefore, smaller-stature transplant candidates (e.g., women and Hispanic/Asian patients) are disadvantaged on the transplant waiting lists (Bernards et al. 2022).

In the current system in the US, the aforementioned donor-recipient compatibility factors are overlooked in ranking patients - but not in allocating livers - in the transplant wait lists because deceased-donor livers are allocated on the basis of medical urgency. A transplant patient has a Model for End-Stage Liver Disease (MELD) score that estimates the probability that a patient

Table 1: Historical Data on Disparities in Access to Liver Transplant. **Likelihood of Transplant (%)** column reports the patients’ likelihood of receiving a transplant relative to the patients with height ≥ 185 cm. Data from UCSF Liver Center.

Height (cm)	Likelihood of Transplant (%)
≤ 150	81
151 - 165	89
166 - 185	93

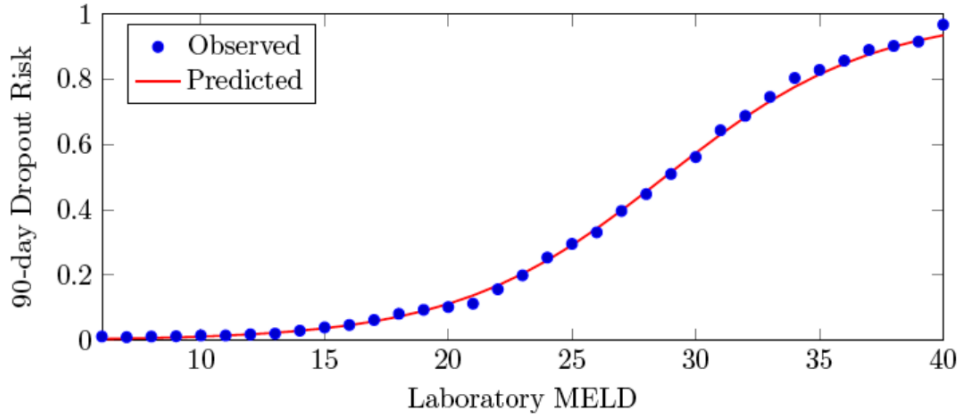
will survive their liver disease during the next three months (Laboratory MELD score vs. 90-day dropout risk curve can be seen in Figure 1). Higher MELD score indicates that a patient needs a liver transplant more urgently. The MELD score of a patient is solely based on a patient’s results from four blood tests²; it is updated more frequently as a patient’s disease progresses (ranges from once a year to once in three months to once a month to once a week). When a deceased-donor liver becomes available, UNOS sequentially offers this liver to the compatible patients who are ranked by their MELD scores after considering their geographical proximity to the donor. The number of offers is limited due to the cold-ischemia time of a liver (i.e. the time before a liver loses its functionality); the liver is discarded if a patient (or a surgeon) does not accept the organ in time.

The MELD score is an excellent predictor of survival for more than 70% patients on the transplant waitlists (Godfrey et al. 2019, Rickert et al. 2019b); however, the severity of the disease of some patients or the risk of complications are not captured by their laboratory MELD scores. Transplant candidates whose MELD scores under-predict their short-term mortality risk apply for a *MELD score exception* to be placed in a higher position on the transplant wait list. These exception scores are widely used in MELD-based allocation of deceased-donor livers; Hepatocellular Carcinoma (HCC) is the most common reason for MELD score exceptions along with 17 group of diagnoses (Asrani and Kamath 2015; Massie et al. 2011).

In this paper, we address the inequity in access to transplantation in the current liver allocation system where disadvantaged patient groups (shorter candidates) experience a longer time until transplantation and have a lower probability of receiving a liver transplant. We model the liver transplant wait list as a multi-class overcrowded queueing system - a class is a patient group based on height (static) and the MELD score (dynamic) - with heterogeneous servers (deceased donors with different liver sizes). We study the first-order fluid approximation of this dynamic stochastic system for tractability. We solve the resulting optimal control problem: the objective is to minimize the pre-transplant mortality of patients over a finite time horizon with an explicit

²MELDNa = $3.78 \times \ln[\text{serum bilirubin (mg/dL)}] + 11.2 \times \ln[\text{INR}] + 9.57 \times \ln[\text{serum creatinine (mg/dL)}] + 6.43 - \text{Na} - [0.25 \times \text{MELD} \times (140 - \text{Na})] + 140$

Figure 1: 90-day mortality risk of ESLD patients



Notes. The logistic regression coefficients can be found in Appendix A.

fairness constraint that equalizes the likelihood of receiving a transplant for all patient groups. We show that the optimal policy, Equity Adjusted Mortality Risk Policy (EAMRP), ranks patients with respect to their medical urgency, as in the current MELD-based allocation, but adjusts this ranking in favor of the disadvantaged patient groups so that all patient groups have equal access to transplantation.

In addition to our theoretical results, we provide a computational method to calculate MELD score exceptions. The *shadow prices* of the optimal control problem can be mapped into the MELD score exceptions for disadvantaged patient groups. Our proposed exception points are closely tied to the patients’ short-term mortality risk while waiting for a transplant. Using these exception scores, we move shorter patients to higher positions in the transplant wait list so that their likelihood of receiving a liver transplant increase. We test the performance of our exception points on a simulation of the national liver allocation system - Liver Simulated Allocation Model (LSAM)- the widely accepted benchmark. We compare the performance of EAMRP with the existing policy and a couple of neighboring static policies (based only on height and not on evolving MELD scores) on various fairness metrics (average time until receiving a transplant, likelihood of transplantation) and efficiency criteria (pre-transplant mortality rate, number of wasted organs, quality-adjusted life years, QALY) across different patient groups as well as the entire system.

By design, all patient groups’ access to transplantation converges to one other. Our simulations show that shorter transplant candidates’ (mostly female and Hispanic patients) likelihood of receiving a liver transplant improves significantly, and as a result, their likelihood of death while waiting for a liver transplant decreases. Their quality-adjusted life years increase and average waiting time until transplantation decrease. As desired, shorter patients materially benefit from receiving

MELD exception points (even the static non-optimal ones) without significantly decreasing the overall efficiency of the system.

The remainder of the paper is organized as follows. In §2, we review the related literature and discuss our contributions. §3 presents the fluid model, the resulting optimal control problem, and the optimal policy for allocating deceased-donor livers. Motivated by our optimal policy, we show how we provide MELD exception points to disadvantaged patient groups in §5. In §6, we present the results of our simulation study to discuss how the equity and efficiency metrics are affected by the introduction of MELD exception points. We conclude the paper and discuss potential research directions in §7.

2 Related Literature

Our work overlaps with and enhances the literature in three areas.

Two-sided matching queues: Organ allocation systems are two-sided markets where heterogeneous supply types (donor organs with different blood types, sizes) are matched with a subset of demand types (patients with different blood types, heights). The queueing papers that study such two-sided markets have considered both rational and myopic agents. In the former rational queueing setup, Afeche et al. (2021) find the optimal design of service compatibility topologies given the trade-off between customers' waiting time delays and maximizing match rewards. For a review of the strategic queueing literature in healthcare, see Akan (2018). Matching queues without incentives are studied by Gurvich and Ward (2015) who focus on finite-horizon cumulative holding costs of items. Similarly, Nazari and Stolyar (2019) propose an optimal matching policy that maximizes long-run average matching rewards while keeping queues stable, and Hu and Zhou (2020) design optimal matching policies that maximize total discounted rewards. In most queueing literature, patient types are static, whereas in organ transplant settings, patients change classes while waiting for a transplant (e.g. health deterioration). This led us to use the first-order fluid approximation. See Alagoz (2008) and Akan et al. (2012) for applications of overloaded fluid models to liver allocation.

Organ allocation. These have been studied extensively by economists and operations researchers. In their early work, David and Yechiali (1985) consider a patient's problem of accepting a kidney offer as a time-dependent stopping problem to maximize their expected reward from transplantation. Richter (1989) models the kidney allocation process as a stochastic assignment problem with the objective of maximizing the total expected reward. Similarly, Ahn and Hornberger (1996) and Howard (2002) solve a transplant patient's problem of accepting/rejecting a kidney offer, and Alagoz et al. (2004, 2007), Said et al. (2009), and Sandikci et al. (2008) consider a patient's

problem for a liver offer. In a series of papers, Su and Zenios (2004, 2005, 2006) study how patient choice impacts the kidney allocation mechanisms. From a geographical perspective, Kong et al. (2010) solve the problem of maximizing the efficiency of the liver allocation system, and Ata et al. (2017) address the region-based inequity in access to kidney transplantation. Bertsimas et al. (2013) propose a data-driven method for designing national policies for kidney allocation with the objectives of fairness and efficiency. Dai et al. (2020) analyze the welfare consequences of introducing donor-priority rule, which grants registered organ donors priority in receiving organs in case they need transplants in the future.

Within this extensive literature, our paper contributes to the stream that focuses on the optimal design of organ allocation policies using the first-order fluid approximation of the transplant system. Zenios et al. (2000) find the best kidney allocation policy with the trade-off between clinical efficiency (i.e. QALY) and equity in access to transplantation, Akan et al. (2012) design optimal liver allocation policies where the trade-off is between medical urgency (i.e. total number of patient deaths) and efficiency, and Hasankhani and Khademi (2021) propose optimal policies of allocating hearts with the trade-off between efficiency and equity. Given the prevalence of medical urgency in the current liver allocation system (i.e. MELD-based allocation), we restrict our focus on improving equity in access to liver transplantation while keeping medical urgency as our objective. In addition to proposing the optimal policy of allocating deceased-donor livers, differently from this stream of literature, we show that the shadow prices of the optimal control problem can be used to estimate transplant patients' short-term mortality risk; hence, we utilize our fluid model to introduce MELD exception points that can be used by policy makers to improve equity within the current MELD-based system.

Exception Points. Medical scientists study the problem of providing novel MELD exception points to patients with HCC whose mortality risks are under-predicted by their MELD scores. Toso et al. (2012) use a proportional hazard model, Vitale et al. (2014) run multivariable regressions, and Marvin et al. (2015) use a Cox regression model to estimate the short-term mortality risk of patients with HCC to provide MELD exception points. Rickert et al. (2019a) demonstrates that HCC patients can be rationally stratified according to medical urgency. Although this literature lacks studies to provide model-based MELD exception points to non-HCC patients (e.g. patients with cystic fibrosis, hepatopulmonary syndrome, etc.), our computational framework of providing MELD exception points can be generalized with non-HCC patients who apply for MELD exception points. Bernards et al. (2022) numerically study static MELD exception points, based only on height and regardless of their laboratory MELD scores, a simplification based on the optimal policy developed in this paper. Our model takes the dynamics of the liver transplant waitlist

(e.g. patients’ health evolution, patient/donor arrivals, mortality, etc.) into account, endogenously calculates transplant patients’ short-term mortality risk that can be directly mapped into MELD score exceptions, and provides different MELD exception points to disadvantaged patients based on candidates’ evolving laboratory MELD scores.

Ruth et al. (1985) and Pritsker et al. (1995) are among the early papers that analyze the kidney and liver allocation systems via simulation, respectively. Kreke et al. (2002) and Shechter et al. (2005) incorporate the patients’ disease evolution, and Kim et al. (2015) develop a machine learning-based model to incorporate transplant patients’ accept/reject decisions into the simulations of the liver allocation system. Davis et al. (2013) and Sandikci et al. (2019) develop discrete-event simulations of the national kidney allocation system to evaluate potential policy changes in kidney allocation. We assess the performance of our outputs - the exception points - of the discretized version of our fluid model using the Liver Simulated Allocation Model (LSAM) developed by Scientific Registry of Transplant Recipients (SRTR) on various equity and efficiency metrics. LSAM is a well-established tool for modeling changes to liver allocation policy and has been used as the basis for previous (cf. Heimbach 2015) and proposed (cf. Rickert et al. 2020 and Bernards et al. 2021) changes to allocation of MELD exception points.

3 A Fluid Model and Analysis

We model the liver transplant waiting list as a multiclass overcrowded queueing system with heterogeneous servers. Given the complex dynamics of this problem (patients’ health evolution, mortality, etc.), we use the first-order fluid approximation of the queueing system to solve for the resulting optimal control problem in finite horizon. We introduce our fluid model with the objective of minimizing patients’ pre-transplant mortality in the system in §3.1, propose our optimal policy and discuss the interpretation of the shadow prices of the optimal control problem in §3.2. Table 2 summarizes our notation. Proofs of our results can be found in Appendix B.

We construct a stylized fluid model to characterize the liver allocation process and to track the dynamics of the system. An overview of this section is as follows. We first describe the ESLD patients and their dynamics while waiting for a liver transplant. Next, we describe the deceased-donor livers being harvested for the transplant patients, control variables that correspond to the allocation of donor livers to patients and the state of the system. Finally, we formulate our objective function as minimizing pre-transplant mortality in finite horizon with fairness constraints for different patient classes to ensure equity in access to transplantation.

We divide ESLD patients who wait for a liver transplant into different classes along two dimensions: static patient characteristics, such as height, and dynamic patient characteristics that

Table 2: Summary of notation

Symbol	Definition
i	Index for the static class of the patient
j	Index for the health status of the patient, i.e., MELD score
k	Index for the type of the donor liver
t	Time index
n	Number of organ offers to patients
\mathcal{I}	Set of static classes of patients
\mathcal{J}	Set of health status of patients, i.e., MELD scores
\mathcal{K}	Set of liver types
Φ	Feasible set of allocations
β	Matrix of patients' health transition rates out of MELD scores
γ	Matrix of patients' health transition rates into MELD scores
ρ	Inverse of the average likelihood of transplantation
λ_{ij}	Arrival rate of class ij patients
μ_k	Arrival rate of type k livers
P^k	Matrix of patients' probability of accepting liver offers
x_{ij}	Number of class ij patients in the system
$\alpha_{jj'}$	Transition rate of a patient's health status from j to j'
d_j	Mortality rate of a patient in health status j
u_{ijk}	The rate of allocating type k livers to class ij patients
INF	Set of incompatible patient type - liver type pairs
p_{ijk}	Probability of a class ij patient accepting an offered liver type of k
π_{ijk}^n	Probability of a type k liver is transplanted into a class ij patient when offered to n patients

represent their health status, i.e., laboratory MELD score. The former dimension is denoted by $i \in \mathcal{I} := \{1, 2, \dots, I\}$ where I is the total number of patient groups, and the latter dimension is denoted by $j \in \mathcal{J} := \{1, 2, \dots, J\}$ where J is the total number of laboratory MELD scores.³ MELD score of a patient may change over time, implying that the patients' dynamic class might change in our model. See Appendix C for a diagram of the class structure of patients with ESLD.

Patients of class ij arrive at the liver transplant waitlist with rate $\lambda_{ij}(t)$ for $t \geq 0$, and the number of class ij patients waiting for transplantation at time t is denoted by $x_{ij}(t)$; initially, there are $x_{ij}(0)$ patients in class ij . As we mentioned earlier, patients' health status (i.e. MELD score) change while waiting for a transplant. In many cases, the patient's health condition deteriorates, leading to an increase in their MELD scores; however, it is also possible for some patients (e.g. patients with primary biliary cirrhosis) to experience a temporary recovery when they first join the waitlist leading to a decrease in their MELD scores. To be specific, we denote the rate at which a patient's MELD score changes from j to j' with $\alpha_{jj'}$ for $(j, j') \in \mathcal{J} \times \mathcal{J}$ without any structural

³In UNOS policy there are 35 dynamic patient classes, i.e. $J = 35$, because MELD score takes integer values between 6 and 40.

assumptions. The rate at which a patient with MELD score j dies while waiting for a transplant is denoted by d_j . Patients with higher MELD scores are more likely to die, therefore, we assume that $d_j > d_{j'}$ for $j > j'$.

A type k deceased-donor liver arrives at the liver transplant system with rate $\mu_k(t)$ for $k \in \mathcal{K} := \{1, \dots, K\}$ and $t \geq 0$. The type of a liver is defined by its blood type and size. We denote the rate at which type k livers are dynamically allocated to class ij patients by $u_{ijk}(t)$ for $i \in \mathcal{I}$, $j \in \mathcal{J}$, $k \in \mathcal{K}$ and $t \geq 0$. The static type of a patient (i.e. height), denoted by i , must be compatible with the liver type k (i.e. size) so that a type k deceased-donor liver can be offered to class ij patients for all $j \in \mathcal{J}$. We ensure this with an incompatibility constraint on the control variables, specifically, $u_{ijk}(t) = 0$ for $(i, k) \in INF$, all $j \in \mathcal{J}$ and $t \geq 0$ where INF contains the incompatible patient type - donor liver type pairs.

Patients have the option of rejecting offered livers due to the expectation of receiving a better organ offer in the future. We denote the probability of a class ij patient accepting a type k liver by p_{ijk} . In our model, a deceased-donor liver can be offered to multiple patients in the waitlist. If a type k liver is offered to n patients of class ij , the probability of the liver being rejected by all patients, i.e. the organ is wasted, becomes $(1 - p_{ijk})^n$. As a result, the probability of a type k liver being transplanted when it is offered to n class ij patients, π_{ijk}^n , becomes $\pi_{ijk}^n = 1 - (1 - p_{ijk})^n$.

The state of the system is denoted by $x(t)$ that keeps track of the number of patients in each patient class at time t , i.e. $x(t) = (x_{11}(t), \dots, x_{ij}(t), \dots, x_{IJ}(t))^T$ for $t \geq 0$. Similarly, we denote the IJ -dimensional vector of control variables for each liver type k by $u^k(t)$ where $u^k(t) = (u_{11k}(t), \dots, u_{ijk}(t), \dots, u_{IJk}(t))^T$ for $k \in \mathcal{K}$ and $t \geq 0$. A feasible control $u(t)$ must satisfy three sets of constraints: (i) the total allocation of type k livers cannot exceed the supply of livers of the same type, (ii) the allocation of deceased-donor livers for incompatible patient - donor type pairs must be zero, and (iii) the allocation of livers for the compatible patient - donor type pairs must be non-negative. Therefore, we define the set of feasible controls, $\Phi(t)$, as follows:

$$u(t) \in \Phi(t) := \{u(t) : e \cdot u^k(t) \leq \mu^k(t); u_{ijk}(t) = 0 \forall j \in \mathcal{J}, (i, k) \in INF; u^k(t) \geq 0\} \quad (1)$$

where e is an IJ -dimensional vector of ones.

Given a feasible control u , the state of the system evolves as follows:

$$\dot{x}(t) = \lambda(t) - \sum_{k=1}^K P^k u^k(t) - (d + \beta - \gamma)x(t), \quad t \geq 0, \quad (2)$$

where P^k is an $IJ \times IJ$ dimensional diagonal matrix with entries π_{ijk} for $i \in \mathcal{I}$, $j \in \mathcal{J}$ and each

liver type $k \in \mathcal{K}$. $\lambda(t)$ is the IJ -dimensional vector of arrival rates of patients, $\lambda_{ij}(t)$, at time t . The square matrix of d has shape $IJ \times IJ$ and it includes the death rate of patients for each MELD score, d_j , in its diagonal entries. Similarly, the square matrices β and γ , obtained from matrix α , include the health transition of the patients in each MELD score. The former, β , contains the rate of health transition of patients from each MELD score to other MELD scores, i.e. it has $\sum_{j \neq j'} \alpha_{jj'}$ and $\alpha_{jj} = 0$ in its diagonal entries for each $j \in \mathcal{J}$. The latter, γ has a shape $IJ \times IJ$, includes the health transition rate of patients into each MELD score from other MELD scores, that is, it has $\alpha_{j'j}$ for each $j \in \mathcal{J}$ in block diagonal matrices of shape $J \times J$. Finally, we require that the number of patients in each class must be non-negative, that is,

$$x(t) \geq 0 \text{ for } t \geq 0. \quad (3)$$

Our aim is to develop MELD exception points for disadvantaged patient groups to ensure their equal access to transplantation. For this reason, we focus on equalizing the likelihood of transplantation measure in all classes of patients with respect to their static characteristics. The following constraint ensures that the ratio of the total amount of deceased donor livers allocated to the total arrival rate of each static patient class must be the same:

$$\int_0^T \sum_{k=1}^K e \cdot u_i^k(t) dt = \frac{1}{\rho} \lambda_i T \text{ for } i \in \mathcal{I}, \quad (4)$$

where $1/\rho$ is the average likelihood of transplantation, $\lambda_i T$ is the total arrival rate of patients of class i , equals to $\int_0^T \sum_j \lambda_{ij}(t)$ over the finite time horizon, and $\int_0^T \sum_{k=1}^K e \cdot u_i^k(t) dt$ gives the total amount of allocated livers to class i patients. In reality, the classes of disadvantaged patients experience a lower likelihood of transplantation, i.e., the value of $1/\rho_i$ for disadvantaged patient class i is lower than the value of $1/\rho_{i'}$ for $i' \in \mathcal{I}$, so we ensure that the likelihood of transplantation is equal for all patients by enforcing the same value, $1/\rho$, independent of static patient classes.

The likelihood of transplant constraint (4) requires the integration of the control variable $u(t)$. We reformulate this constraint by introducing another state variable $w(t)$ where $w_i^k(0) = 0$ and

$$w_i^k(t) = \int_0^t e \cdot u_i^k(\tau) d\tau, \dot{w}_i^k(t) = e \cdot u_i^k(t) dt \text{ for } k \in \mathcal{K}, t \geq 0. \quad (5)$$

The state variable $w_i(t)$ captures the number of livers of all types allocated to static type i patient across all MELD values j . Requiring $w_i(T)$ to be proportional to the total arrivals $\lambda_i T$, we can

express the equity constraint (4) equivalently as a terminal condition:

$$\sum_{k=1}^K w_i^k(T) = \frac{1}{\rho} \lambda_i T \text{ for } i \in \mathcal{I}. \quad (6)$$

We reflect the current liver allocation policy that prioritizes medical urgency (MELD-based allocation) with our objective function of minimizing pre-transplant mortality of patients while waiting for a liver transplant. Since patients with higher MELD scores have a higher mortality rate, this objective ensures that they are prioritized over patients with lower MELD scores when receiving liver transplant offers. As a result, the problem of minimizing pre-transplant mortality with equity constraints becomes one of choosing an organ allocation policy $\{u(t) : 0 \leq t \leq T\}$ to

$$\text{minimize } \int_0^T (e \cdot d) \cdot x(t) dt \quad \text{subject to (1) - (3) and (5) - (6),} \quad (\text{P})$$

with the initial state of the system $x(0) = x_0$ and $w(0) = 0$. We discuss the estimation of model (P) parameters in Section 6.

4 Dual problem formulation and the proposed policies

In this section, we first present the dual problem formulation (D) of our optimal control problem (P), and the coextremality results between the two formulations. Next, we describe the implementation of the optimal policy, named Equity Adjusted Mortality Risk Policy, from a policy maker's perspective. Finally, we provide the interpretation of the shadow prices from the dual problem that lays the foundation for our computational framework of providing MELD exception points to disadvantaged patient groups.

The dual problem of control associated with the problem (P) of maximizing QALY can be stated as follows (see Appendix B for its derivation): Choose IJ dimensional processes $\{y(t), z(t) : 0 \leq t \leq T\}$ and $q_i : i \in \mathcal{I}$ so as to minimize

$$\int_0^T [y(t)\lambda(t) + f(t, y(t), z(t))]dt + x(0) \cdot y(0) - \frac{z(T)\lambda T}{\rho}$$

subject to

$$\begin{aligned} y(t) &= y(0) + \int_0^t \dot{y}(s)ds \\ z(t) &= \int_0^t \dot{z}(s)ds \\ \dot{z}(t) &= 0 \\ \dot{y}(t) &\leq y(t)(d + \beta - \gamma) + d \end{aligned} \tag{D}$$

where $f(t, y(t), z(t)) = \inf \sum_{k=1}^K \{(y(t) \cdot P^k - z(t))u^k : u(t) \in \Phi(t)\}$.

In the dual formulation, the state vector $y_{ij}(t)$ is the shadow price that corresponds to the ij^{th} system evolution constraint (2) in the primal problem (P), $z_i^k(t)$ is the ik^{th} shadow price corresponding to the evolution of the control variable u , i.e. $\dot{w}_i^k(t) = u_i^k(t)dt$, and q_i is the i^{th} shadow price corresponding to the likelihood of transplant constraint for patient class i .

The dual problem (D) and the primal problem (P) are closely linked to each other. Above all, the objective function values of (P) and (D) are equal. Moreover, any optimal primal solution and any optimal dual solution satisfy a set of coextremality conditions, which are necessary and sufficient conditions for optimality. The following result summarizes the duality results between the two formulations that are relevant for our purposes; its proof is given in the Appendix B.

Theorem 1 *The primal problem (P) of minimizing pre-transplant mortality and the dual problem (D) have the same objective value. Furthermore, letting u and (y, z) pair be a feasible organ allocation policies for (P) and (D), the primal control u and the dual control (y, z) are optimal for (P) and (D), respectively, if and only if they satisfy the coextremality conditions given below. For $i \in \mathcal{I}$, $j \in \mathcal{J}$ and $t \in [0, T]$,*

$$\dot{y}_{ij}(t) = d_{ij} + [y(t)(d + \beta - \gamma)]_{ij} \text{ if } x_{ij}(t) > 0, \tag{7}$$

$$\dot{z}(t) = 0, z(T) = \frac{q}{\rho}\lambda T, \tag{8}$$

$$u^k(t) \in \arg \min_{v \in \Phi(t)} \{(P^k \cdot y(t) - z(t))v^k\} \text{ for } k \in \mathcal{K}. \tag{9}$$

Equity Adjusted Mortality Risk Policy. Motivated by Theorem 1, we next propose our policy to maximize the total quality adjusted life years of all patients with ESLD, the ultimate goal of the liver allocation system. The policy is named the Equity Adjusted Mortality Risk Policy, because not only does it minimize overall waitlist deaths but also minimize the gap between

transplant rates across patient groups. Hence, it truly captures the goal of equity for each possible allocation decision.

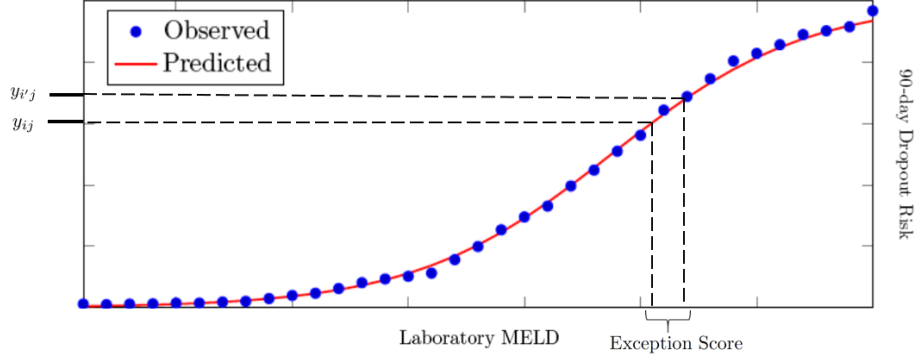
Theorem 1 characterizes the optimal allocation of deceased-donor livers via Equation (8). When a liver of type k arrives at time t , a policy maker ranks patients in class ij with respect to the quantity $y_{ij}(t)\pi_{ijk}^n - z_i(t)$ where the number of parallel organ offers is n and class ij patients' probability of accepting the liver offer is π_{ijk}^n . With the objective function of minimizing pre-transplant mortality, the dual state variable $y_{ij}(t)$ gives the potential increase in the objective function if we were to increase the number of patients in class ij by one, in other words, it gives us the mortality risk of an additional patient of class ij at the end of the time horizon. The dual state variable $z_i(t)$ gives the potential decrease in the objective function if we were to increase the likelihood of transplant of class i patients by 1%, i.e., it gives us the mortality risk of class i patients that can be avoided by increasing their access to transplantation. Therefore, the Equity Adjusted Mortality Risk Policy non-decreasingly orders patients in terms of their adjusted mortality risk to allocate deceased-donor livers to the ESLD patients.

In the current liver allocation system, transplant patients are prioritized with respect to their medical urgency, i.e. MELD score, and their access to transplantation is not considered as a factor while allocating deceased-donor livers. This is reflected in the first term of the optimal policy, $y_{ij}(t)\pi_{ijk}^n$, in the absence of fairness constraints for a fixed patient class i . Since patients with higher MELD scores have a higher mortality risk, i.e. $y_{ij}(t) < y_{ij'}(t)$ for $j < j'$ and $t \in [0, T]$, and have a higher probability of accepting incoming liver offers, i.e. $\pi_{ijk}^n < \pi_{ij'k}^n$ for $j < j'$, a policy maker offers a transplant organ to patients of class i starting from the patients with the highest MELD score. Adding the fairness constraints to the primal problem (P) brings a new term, $z_i(t)$, that allows for the case where a disadvantaged patient with a relatively better health status, i.e. lower laboratory MELD score, might be prioritized to increase their access to transplantation.

5 Providing MELD Exception Points

In this section, we describe a general framework to achieve equity by providing exception points to disadvantaged groups. First, we establish the connection between the dual state variables of the optimal control problem and MELD exception points. Then, we provide an easy-to-implement algorithm to provide exception points by using parameter estimates. Finally, we demonstrate a numerical example to explain how MELD score exceptions would be provided to disadvantaged patient groups by the policy makers in practice. Our framework is quite general and can also be used in other point-based allocation systems (e.g., social housing, child adoption) where equity is an important concern.

Figure 2: MELD Exception Point on Laboratory MELD - 90-day Mortality Risk Curve



For ease of discussion, we consider patients in two static classes where i represents the regular class and i' represents the disadvantaged patient class with lower likelihood of receiving a liver transplant. As we have seen in the previous section, the dual state variable that corresponds to the ij th system evolution constraint (2) in the primal problem (P), $y_{ij}(t)$, gives us the mortality risk of a class ij patient at the end of the time horizon for $i \in \mathcal{I}$, $j \in \mathcal{J}$ and $t \in [0, T]$. We solve (P) by replacing $1/\rho$ with $1/\rho_i$ for class i patients and $1/\rho_{i'}$ for class i' patients in constraint (4). This gives us $y_{ij}(t)$ for a patient who belongs to the regular class with MELD score j and $y_{i'j}(t)$ for a patient who belongs to the disadvantaged class with the same MELD score where $y_{ij}(t) < y_{i'j}(t)$ because the likelihood of receiving a transplant for a class i patient, $1/\rho_i$, is greater than for a class i' patient, $1/\rho_{i'}$. The closest integer to the inverse of the difference between $y_{ij}(t)$ and $y_{i'j}(t)$ on the MELD score - short-term mortality risk curve becomes the MELD score exception point for the class $i'j$ patient. Figure 2 visualizes the MELD exception points for the disadvantaged patients in class i' at MELD score j .

The primal optimal control problem (P) is linear with respect to the state variable x and the control variable u , therefore, the discretized version of it turns out to be a linear program that can be efficiently solved using parameter estimates. The dual state variable y can also be easily extracted from the primal problem letting us to provide MELD exception points to disadvantaged patient groups. Given the parameter estimates of the primal problem, Algorithm 1 is easy to use by a policy maker who aims to increase disadvantaged patient groups' access to transplantation. The parameter estimates include the initial state of the system, i.e. the number of patients in each class x_0 , the average arrival rate of patients into the transplant waitlist, λ , the average arrival rate of deceased-donor livers, μ , the transplant acceptance probability of patients in each class, P , the rate of health transitions of patients in each MELD score, α , the mortality risk of patients, d , the feasible set of organ allocations, Φ , and the average likelihood of transplantation of each patient

Algorithm 1 Providing MELD Exception Points

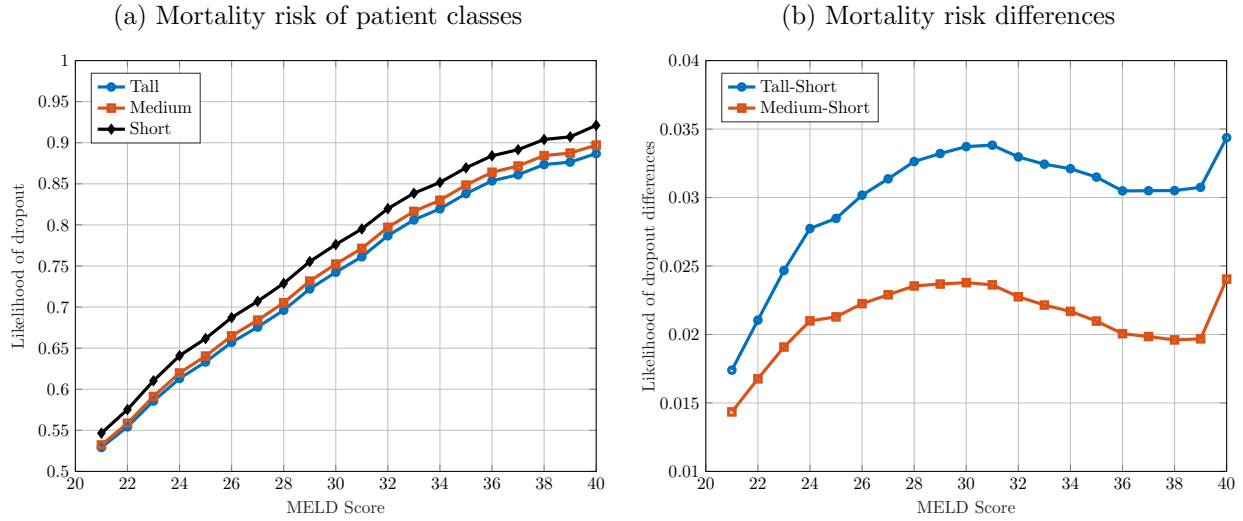
Require: $x_0, \lambda, \mu, P, \alpha, d, \Phi, 1/\rho$
discretize the time horizon;
solve the resulting Linear Program (LP);
for Patient class pairs (i,i') **do**
 for MELD score j **do**
 if $y_{i'j} > y_{ij}$ **then**
 $j' \leftarrow$ inverse of $d_j + y_{i'j} - y_{ij}$ on MELD - 90-day mortality risk curve
 Exception Point $_{i'j} \leftarrow \lfloor j' - j \rfloor$
 end if
 end for
end for

class, $1/\rho$. We note that the historical data or the forecasts for a pre-specified time horizon (3 months, 1-year) can be used to estimate parameters such as average arrival rates and likelihood of receiving a liver transplant. After the linear program is solved using the estimated parameters, one can check the dual values of each patient class corresponding to the system dynamics constraints at each MELD score, and give the exception points to the disadvantaged patient groups whose dual values appear to be higher than other patient groups.

For the numerical demonstration, we use the data from UNOS Region 5, which includes the states of Arizona, California, Nevada, New Mexico and Utah, for the years between 2012 and 2017 to estimate transplant patient and deceased-donor arrival rates. We abstract away the blood type matching and focus only on the size matching to classify patients into different groups with respect to their heights. As we mentioned earlier, shorter patients can receive transplantation from a smaller pool of available donors, i.e., only small size deceased-donor livers, compared to medium-height and tall patients. As in Lai et al. (2010), we consider patients taller than 180 cm as tall, between 165-180 cm as medium-height, and shorter than 165 cm as short patients. The primal optimization problem (P) is solved for a varying set of different time horizons, and the results from the 1-year horizon are presented for brevity. Figure 3 shows the dual values that are endogenously calculated from the primal problem, i.e., tall, medium and short patients' mortality risk at each MELD score, and the differences between dual values of all patient class pairs.

Figure 3(a) shows us that the mortality risk of all patients for low MELD scores, i.e. < 20 , are very close to each other regardless of their height because ESLD patients rarely receive transplantation when their health condition is relatively well. We do not provide exception points to short patients in this interval. The patients in the transplant waitlist receive deceased-donor liver offers for the MELD scores higher than 20; therefore, we observe the discrepancy between the short, medium-height and tall patients' mortality risks for higher MELD scores due to the differences in

Figure 3: Estimated Mortality Risk of Transplant Patients in Region 5



their access to transplantation. Using the differences in the mortality risk of patients in Figure 3(b), we provide MELD score exception points to short patients. For MELD scores between 21 and 34, the difference between the mortality risk of tall and short patients grants +1 exception point to short patients to artificially move them to higher positions in the transplant waitlist. For MELD scores between 35 and 38, short patients are granted +2 exception points because the difference between the mortality risks corresponds to a higher MELD score difference on laboratory MELD score - short-term mortality risk curve. Medium-height patients do not qualify for MELD score exceptions because the difference between their their mortality risk and tall patients' is not high enough for them to be granted. These exception points improve short patients' access to transplantation to decrease their mortality risk while waiting for a liver transplant.

6 Simulation Results

In this section, we present the results from the simulations of the national liver allocation system to study how various efficiency and equity metrics are affected by our proposed MELD score exception points to disadvantaged patient groups. First, we introduce the simulation model and describe the system dynamics that are updated over the course of the simulation. Second, we explain how our computational procedure is incorporated into the simulations to compute MELD exception points. Then, we present the simulation results on equity with our proposed exception points and compare the potential improvement over the current policy and static exception points. Improving equity of a system comes at the cost of losing efficiency in general; therefore, we present the simulation results on efficiency metrics for each individual patient group as well as the overall system. Finally, we

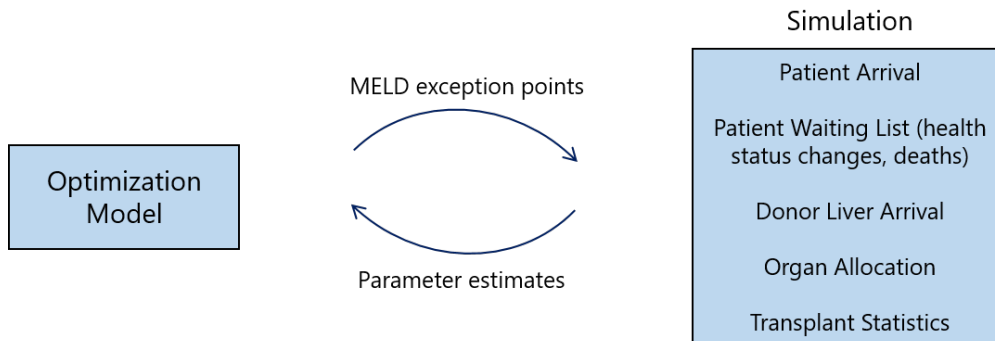
discuss how the trade-off between efficiency and equity is affected by our proposed MELD exception points.

We use the Liver Simulated Allocation Model (LSAM), a computer simulation program developed by the Scientific Registry of Transplant Recipients (SRTR), to simulate the allocation of livers to candidates on the Organ Procurement and Transplantation Network (OPTN) waiting list. A more detailed description of the simulation model and its validation can be found in SRTR (2019). The current liver allocation system consists of 11 regions and 58 donor service areas (DSA). When transplant candidates arrive at a particular DSA, they are assigned a laboratory MELD score, blood type, Status 1 exception (for critically ill patients), and HCC exception. In addition to the aforementioned exception points that are provided by LSAM, we provide MELD exception points to patients based on their height and laboratory MELD score. During the simulation, transplant candidates' laboratory MELD scores are updated reflecting the changes in their health status, and they are removed from the waitlist due to death or other reasons (e.g. being medically unsuitable for transplantation). After a deceased donor arrives, the liver is assigned a blood type with donor's height information and it is offered to blood type and size-compatible candidates in accordance with the current allocation policies. The patient preferences module computes the acceptance probability of each transplant candidate when a deceased-donor liver becomes available, and the organ is discarded if it is rejected by all candidates who receive an offer. Lastly, the transplant statistics module computes the related performance metrics of the overall system that we discuss later in this section.

In our simulation study, we purely focus on providing MELD score exception points based on transplant recipients' height. Extending the example based on three height groups in §5, we divide transplant patients into five height tiers (≤ 150 cm, 151-156 cm, 157-165 cm, 166-175 cm, ≥ 176 cm) that align with the medical literature on liver transplantation (Bernards et al. 2022). In order to capture more granular differences in the most disadvantaged patients, shortest patients are split into smaller tiers compared to tall patients. The data of transplant candidates and donors are collected from LSAM input files for the study period of July 1, 2011 to June 30, 2016. We run LSAM simulations of the current policy and our proposed policy for a 5-year horizon with 3 replications. The average results are presented in this section for brevity.

The interaction between the simulation of the national liver allocation system and our optimization model is visualized in Figure 4. For a 1-year period, our simulation runs with the UNOS' current policy of allocating livers based on medical urgency to estimate each patient group's likelihood of receiving a liver transplant. Along with the estimated rates of patient and donor liver arrivals, and waiting list dynamics, these parameters are used in our optimization model to endoge-

Figure 4: Optimization Model and Simulation: (a) Parameter Estimates are obtained from LSAM for the Optimization. (b) Exception Points calculated are simulated in LSAM.



nously compute the mortality risk of patients that result in MELD score exception points for short patients in Algorithm 1. These exception points are then fed into the simulation to evaluate the changes in the performance metrics. In case there are still discrepancies between different patient classes in terms of their likelihood of transplantation, we repeat the steps that we have described so far until each patient group’s likelihood of transplantation converge to each other sufficiently.

We define size-based compatibility in deceased-donor liver transplantation with respect to the transplant recipients’ and donors’ heights by using the Body Surface Area Index (BSA_i) thresholds in Fukazawa and Nishida (2016). Body Surface Area Index (BSA_i) of a patient-donor pair is the ratio of a donor’s Body Surface Area (BSA)⁴, correlated to the liver size, to a recipient’s BSA , correlated to the available abdominal volume. A donor liver is considered ”small-for-size” where $BSA_i < 0.78$, and ”large-for-size” where $BSA_i > 1.24$. In order to calculate an average compatibility metric based on available data, we analyze the BSA distribution of deceased donors and transplant recipients. Given $BSA_{\text{Recipient}}$, we first calculate what percent of BSA_{Donor} falls into the compatibility interval, i.e., $0.78 * BSA_{\text{Recipient}} < BSA_{\text{Donor}} < 1.24 * BSA_{\text{Recipient}}$. For each height tier of recipients, we replace $BSA_{\text{Recipient}}$ with $BSA_{\text{Recipient LB}}$ ($BSA_{\text{Recipient UB}}$) in the lower (upper) bound of the interval where $BSA_{\text{Recipient LB}}$ ($BSA_{\text{Recipient UB}}$) is the 5th (95th) percentile of the BSA of transplant patients. Since using $BSA_{\text{Recipient LB}}$ and $BSA_{\text{Recipient UB}}$ gives optimistic estimates for compatibility, we also calculate what percent of $BSA_{\text{Recipient}}$ falls into the compatibility interval given BSA_{Donor} , i.e., $0.78 / BSA_{\text{Donor}} < 1 / BSA_{\text{Recipient}} < 1.24 / BSA_{\text{Donor}}$. This time, we replace BSA_{Donor} with $BSA_{\text{Donor UB}}$ ($BSA_{\text{Donor LB}}$) in the lower (upper) bound of the interval where $BSA_{\text{Donor UB}}$ ($BSA_{\text{Donor LB}}$) is the 95th (5th) percentile of the BSA of donors. The minimum of the compatibility percentage obtained from the first set of intervals and the second set of intervals is taken as the size-based compatibility metric in the optimization model. The resulting compatibility percentages as well as the histogram of donor and recipient $BSAs$ can be found in Appendix D.

⁴ $BSA = 0.007184 * \text{Height}^{0.725} * \text{Weight}^{0.425}$

In order to examine the effect of MELD score exception points to the equity of liver transplantation, we measure the likelihood of receiving a transplant, likelihood of death while waiting for a transplant, and the ratio of likelihood of transplant to the sum of likelihood of death and transplant metrics of each patient group. We compare the performance of our policy with three benchmarks; current UNOS policy without exception points, (1,1,0) policy that grants +1 point to ≤ 150 cm patients and +1 point to 151-156 cm patients with no exception points to remaining patients, and (2,1,0) policy that grants +2 points to ≤ 150 cm patients and +1 point to 151-156 cm patients with no exception points to remaining patients. We call (1,1,0) and (2,1,0) policies as static policies because the exception points are granted to shorter patients based only on height (that is unchanging) regardless of their laboratory MELD score that can evolve. Recall that as is the case in the example discussed in §4, our optimal exception points depend on patients' MELD score as well.

The results on equity with the current UNOS policy, (1,1,0) and (2,1,0) static policies and our policy are presented in Table 3. As discussed in §1, ≤ 150 cm and 151-156 cm candidates have significantly lower likelihood of receiving a deceased-donor liver transplant (35.9% and 37.5%, respectively) compared to 157-165 cm (39.2%), 166-175 cm (40.1%), and ≥ 176 cm (41.0%) candidates with the current policy. Also, the likelihood of death while waiting for a liver transplant is higher for ≤ 150 cm and 151-156 candidates (10.7% and 10.6%, respectively) compared to 157-165 cm (9.6%), 166-175 cm (9.2%), and ≥ 176 cm (8.6%) candidates. Consequently, ≤ 150 cm and 151-156 cm candidates have lower transplant over death plus transplant percentage (77.0 % and 77.9%, respectively) compared to 157-165 cm (80.3%), 166-175 cm (81.3%), and ≥ 176 cm (82.7%) candidates.

(1,1,0) and (2,1,0) static policies improve ≤ 150 cm and 151-156 cm candidates' access to liver transplantation; ≤ 150 cm and 151-156 cm candidates' likelihood of transplant increases to 38.1% and 39.5% with (1,1,0) policy, and to 39.5% and 39.4% with (2,1,0) policy, respectively. These two policies results in a decrease in ≤ 150 cm and 151-156 cm candidates' likelihood of death while waiting for a transplant; ≤ 150 cm and 151-156 cm candidates' likelihood of death drops to 10.5% and 10.1% with (1,1,0) policy, and to 10.2% and 10.1% with (2,1,0) policy, respectively. Our dynamic policy further improves ≤ 150 cm and 151-156 cm candidates' access to transplantation compared to (1,1,0) and (2,1,0) policies; Table 3 shows that ≤ 150 cm and 151-156 cm patients' likelihood of transplant increases to 39.7% and 39.7%, respectively. We also observe a further decrease in 151-156 cm candidates' likelihood of death (9.9%) with our policy compared to (1,1,0) and (2,1,0) policies. Overall, all candidate groups' likelihood of transplant percentages converge to each other with our policy ensuring equal access to deceased-donor liver transplantation.

Table 3: Simulation Results on Equity. Current Policy does not consider height. Our Policy is dynamic, depending on height and MELD score. The (1,1,0) and (2,1,0) policies are static, considering only height but not the evolving MELD score.

Height (cm)	Current Policy	(1,1,0) Policy	(2,1,0) Policy	Our Policy
Likelihood of Transplant (%)				
≤ 150	35.9	38.1	39.3	39.7
151-156	37.5	39.5	39.4	39.7
157-165	39.2	38.9	39.3	39.6
166-175	40.1	39.7	39.7	39.7
≥ 176	41.0	40.4	40.2	40.0
Likelihood of Death (%)				
≤ 150	10.7	10.5	10.2	10.2
151-156	10.6	10.1	10.1	9.9
157-165	9.6	9.8	9.8	9.8
166-175	9.2	9.1	9.2	9.2
≥ 176	8.6	8.8	8.8	8.9
Transplant/(Death + Transplant) (%)				
≤ 150	77.0	78.4	79.4	79.7
151-156	77.9	79.6	79.6	80.0
157-165	80.3	79.9	80.0	80.2
166-175	81.3	81.4	81.2	81.2
≥ 176	82.7	82.1	82.0	81.8

The MELD score exception points for disadvantaged patient groups improve equity in access to liver transplantation. Since improving equity of a system comes at the cost of losing efficiency in general, we use various efficiency metrics to assess the effect of proposed MELD score exception points on the performance of the liver allocation system. In particular, we use the expected quality-adjusted life years of each patient group (QALY), number of wasted livers from each donor group (NWL), number of patients died while waiting for a liver transplant (NPD), and the average waiting time of each patient group until receiving a transplant (AWT).

The percentage improvements in the efficiency metrics over the current UNOS policy are presented in Table 4. As expected, ≤ 150 cm and 151-156 cm candidates benefit from receiving MELD exception points because all performance metrics improve for them. In particular, QALY and AWT objectives for ≤ 150 cm (16.8% and 11.2%, respectively) and 151-156 cm candidates (7.1% and 3.4%, respectively) improve substantially. The decrease in these two objectives is low for 157-165 cm (-1.1% and -0.1%, respectively) and 166-175 cm (-0.7% and -0.3, respectively) candidates compared to ≥ 176 cm candidates (-1.9% and -3.9%, respectively). Similarly, NPD objective for ≤ 150 cm (5.9%) and 151-156 cm (2.1%) candidates improve even though this % improvement is not

Table 4: Simulation Results on Efficiency

Height (cm)	% Difference of Dynamic Policy over the Current Policy			
	QALY	NPD	AWT	NWL
≤ 150	16.8	5.9	11.2	4.1
151-156	7.1	2.1	3.4	1.2
157-165	-1.1	-1.0	-0.1	0.2
166-175	-0.7	-2.2	-0.3	-0.4
≥ 176	-1.9	-3.1	-3.9	-1.1
Total	0.2	-0.1	0.9	-0.6

Notes. QALY: quality-adjusted life years, NPD: number of patients died while waiting for a transplant, AWT: average waiting time until transplant, NWL: number of wasted livers. Note that % difference is considered an improvement when the QALY objective increases; for NPD, AWT, and NWL objectives, we need a decrease to consider it as an improvement. Thus, Dynamic Policy improves every metric for ≤ 150 cm and 151-156 cm candidates as well as the overall QALY and AWT metrics while overall NPD and NWL metrics worsen slightly.

as high as QALY and AWT objectives. This objective becomes worse for 157-165 cm (-1.0%), 166-175 cm (-2.2%), and ≥ 176 cm (-3.1%) candidates. On the supply side, NWL objective improves for ≤ 150 cm (4.1%), 151-156 cm (1.2%), and 157-165 cm (0.2%) donors with a decrease in 166-175 cm (-0.4%) and ≥ 176 cm (-1.1%) donors. Overall, our simulations show that the performance of the liver allocation system improves for QALY, and AWT objectives (0.2% and 0.9%, respectively) whereas NPD and NWL objective worsen slightly (-0.1% and -0.6%, respectively) with our policy. These results suggest that we can improve equity by introducing MELD exception points to disadvantaged candidates without sacrificing the efficiency of the liver transplant system.

Finally, Table 5 presents the change in various equity and efficiency metrics with respect to the patients' gender and race. The shortest stature candidates (≤ 150 cm and 151-156 cm) who receive MELD exception points in our policy represents a disproportionately female and Hispanic proportion of the liver transplant candidate population. Female candidates have a lower probability of receiving a liver transplant, and a higher likelihood of death while waiting for a transplant (38.9% and 9.6%, respectively) compared to male candidates (40.3% and 8.8%, respectively) with the current policy. Hispanic candidates also have lower rates of liver transplant (38.3%), longer waiting times until receiving a transplant (296 days), and higher rates of death (10.9%) in comparison to non-Hispanic candidates (e.g., Caucasian candidates have a transplant rate of 39.4%, an average waiting time of 271 days, and a dropout rate of 9.1%). Our policy almost equalizes female and male candidates' likelihood of liver transplantation (39.8% and 39.9%, respectively) while lowering female candidates' average waiting time until transplantation (from 257 to 256 days), and likelihood

Table 5: Simulation Results on Recipients’ Gender and Race. Our Policy narrows the difference between Women and Men, as well as the disparity between races.

Gender	Current Policy			Our Policy		
	LT (%)	AWT	Death (%)	LT (%)	AWT	Death (%)
Women	38.9	257	9.6	39.8	256	9.4
Men	40.3	277	8.8	39.9	274	8.9
Race/Ethnicity						
Caucasian	39.4	271	9.1	39.2	275	9.2
Hispanic	38.3	296	10.9	38.7	289	10.6
African American	46.4	216	7.6	46.3	218	7.5
Asian	40.1	288	5.7	40.6	269	5.9

of death (from 9.6% to 9.4%). Hispanic (38.7%) and Asian candidates’ (40.6%) transplant rate increases, average waiting time until transplantation decreases (289 and 269 days, respectively), and Hispanic candidates’ likelihood of death (10.6%) decreases with our MELD exception points. Altogether, our simulations demonstrate that disadvantaged candidates (female and Hispanic) greatly benefit from our policy, and more equal rates of liver transplantation and death across the entire transplant candidate population are obtained with MELD exception points.

7 Conclusion

We study the problem of achieving a fairer liver allocation system where there are disparities in access to transplantation based on patients’ height. Shorter patients (who are disproportionately women) have higher average waiting times and mortality rates compared to other patient groups because they can receive liver transplants from a smaller pool of available deceased donors. To address this inequity, (i) we develop a fluid model of the liver transplant system with fairness constraints, (ii) derive the optimal policy of allocating deceased-donor livers to transplant patients, (iii) provide a computational approach to calculate MELD score exception points to disadvantaged patient groups to increase their access to transplantation, and (iv) run simulations of the national liver allocation system (LSAM) to assess the performance of our proposed MELD exception points on the efficiency and equity of the current policy of allocating livers which is based on transplant patients’ medical urgency.

Our analysis shows that the Equity Adjusted Mortality Risk Policy, which ranks transplant patients in terms of their medical urgency, but adjusts this ranking to ensure that all patient groups have equal access to transplantation, is optimal in allocating deceased-donor livers. Without the fairness constraints, we show that the optimal policy coincides with the UNOS’ current policy of

allocating donor livers based on ESLD patients' medical urgency, i.e., ranking patients with respect to their laboratory MELD scores. With fairness constraints, the dual state variables are endogenously calculated while solving the primal optimal control problem of minimizing pre-transplant mortality. We show that these dual variables are a proxy for transplant patients' short-term mortality risk which can be mapped into laboratory MELD scores. With an easy-to-implement algorithm, we utilize real data and provide MELD exception points to disadvantaged patient groups because their short-term mortality risks are higher than those of other patient groups. These exception points move disadvantaged patients to higher positions on the transplant waiting list to improve their access to transplantation.

We run simulations of the national liver allocation system to test the effect of introducing MELD exception points on various efficiency and equity objectives. Our simulations show that disadvantaged patients can greatly benefit from receiving MELD score exceptions without decreasing the efficiency of the overall liver transplant system. Unlike other proposals that require more drastic policy changes, our approach provides a remedy within the current liver allocation system where the transplant patients are prioritized based on medical urgency and the use of exception points is also in use for other situations. In addition to the static patient characteristics that we have discussed in our work (height, gender, race), our methodology can be generalized with any factor that creates discrepancies in organ access. In addition, our shadow price approach can be used to compare medical urgency across organs for patients who need dual organ transplants (a new liver and another new organ during the same surgical procedure), since these patients are listed on both organ waiting lists.

We close by listing other potential considerations that are beyond the scope of this paper. First, we have solely focused on the allocation of deceased-donor livers, therefore, we do not consider living donor liver transplantation in our theoretical and computational analysis. The reasons for this are: (i) living donor liver transplants constitute a small portion (5.5% in 2020) of liver transplants in the US, and (ii) most living donors donate a portion of their healthy livers to their family members or friends without participating in the national liver allocation system. Second, our model and analysis do not incorporate split liver transplants (SLT) which can potentially reduce disparities in organ access due to size mismatch between the donor and the recipient. The practice of splitting deceased-donor livers provides liver transplants for two recipients (in general, one adult and one pediatric patient); however, only 3.8% of all deceased-donor livers are used for SLTs from 2010 to 2015 (Tang et al. 2021). Given their increasing trends in recent years, how to incorporate living donor liver transplants and SLTs into the MELD-based liver allocation system is an interesting research question to study in the future.

References

- Ahn JH, Hornberger JC (1996) Involving patients in the cadaveric kidney transplant allocation process: A decision-theoretic perspective. *Management Science*, 42(5):629-641.
- Akan, M. (2018). Queueing Games. In Handbook of Healthcare Analytics, T. Dai (Ed.). pp. 355-380. <https://doi.org/10.1002/9781119300977.ch16>
- Akan M, Alagoz O, Ata B, Erenay FS, Said A (2012) A broader view of designing the liver allocation system. *Operations research*, 60(4):757-770.
- Alagoz O, Maillart LM, Schaefer AJ, Roberts MS (2004) The optimal timing of living-donor liver transplantation. *Management Science*, 50(10):1420-1430.
- Alagoz O, Maillart LM, Schaefer AJ, Roberts MS (2007) Choosing among living-donor and cadaveric livers. *Management Science*, 53(11):1702-1715.
- Alagoz, O., M. Akan, B. Ata., F.S. Erenay, (2008) "A Fluid Dynamic Model to Optimize the Liver Allocation System" Proceedings of 2008 NSF Engineering Research and Innovation Conference, Knoxville, TN.
- Asrani SK, Kamath PS (2015) Model for end-stage liver disease score and MELD exceptions: 15 years later. *Hepatology International*, 9(3):346-354.
- Ata B, Skaro A, Tayur S (2017) OrganJet: Overcoming geographical disparities in access to deceased donor kidneys in the United States. *Management Science*, 63(9):2776-2794.
- Bernards S, Lee E, Leung N, Zhao H, Akan M, Sarkar M, Tayur S, Mehta N. (2021) Liver Simulated Allocation Model (LSAM) of a Height-Based Policy Change to Improve Sex Disparity in Liver Transplantation (LT) [abstract]. *Am J Transplant*; 21 (suppl 3).
- Bernards S, Lee E, Leung N, Akan M, Gan K, Zhao H, Sarkar M, Tayur S, Mehta N (2022) Awarding additional MELD points to the shortest waitlist candidates improves sex disparity in access to liver transplant in the United States. *American Journal of Transplantation*, 1-9.
- Bertsimas D, Farias VF, Trichakis N (2013) Fairness, efficiency, and flexibility in organ allocation for kidney transplantation. *Operations Research*, 61(1):73-87.
- Cox-North P, Doorenbos A, Shannon SE, Scott J, Curtis JR (2013) The transition to end-of-life care in end-stage liver disease. *Journal of Hospice & Palliative Nursing*, 15(4):209-215.

- Dai T, Zheng R, Sycara K (2020) Jumping the line, charitably: Analysis and remedy of donor-priority rule. *Management Science*, 66(2):622-641.
- David I, Yechiali U (1985) A time-dependent stopping problem with application to live organ transplants. *Operations Research*, 33(3):491-504.
- Davis A, Mehrotra S, Friedewald J, Ladner D (2013) Characteristics of a simulation model of the national kidney transplantation system. *In 2013 Winter Simulations Conference*, 2320-2329.
- Godfrey EL, Malik TH, Lai JC, Mindikoglu AL, Galván NTN, Cotton RT, O'Mahony CA, Goss JA, Rana A (2019) The decreasing predictive power of MELD in an era of changing etiology of liver disease. *American Journal of Transplantation*, 19(12):3299-3307.
- Gurvich I, Ward A (2015) On the dynamic control of matching queues. *Stochastic Systems*, 4(2):479-523.
- Hasankhani F, Khademi A (2021) Is it Time to Include Post-Transplant Survival in Heart Transplantation Allocation Rules?. *Production and Operations Management*, 30(8):2653-2671.
- Heimbach, J. K., Hirose, R., Stock, P. G., Schladt, D. P., Xiong, H., Liu, J., Olthoff, K. M., Harper, A., Snyder, J. J., Israni, A. K., Kasiske, B. L. and Kim, W. R. (2015), Delayed hepatocellular carcinoma model for end-stage liver disease exception score improves disparity in access to liver transplant in the United States. *Hepatology*, 61: 1643-1650. <https://doi.org/10.1002/hep.27704>
- Howard DH (2002) Why do transplant surgeons turn down organs?: A model of the accept/reject decision. *Journal of Health Economics*, 21(6):957-969.
- Kilambi V, Bui K, Mehrotra S (2018) LivSim: an open-source simulation software platform for community research and development for liver allocation policies. *Transplantation*, 102(2).
- Kim SP, Gupta D, Israni AK, Kasiske BL (2015). Accept/decline decision module for the liver simulated allocation model. *Healthcare Management Science*, 18(1):35-57.
- Kong N, Schaefer AJ, Hunsaker B, Roberts MS (2010) Maximizing the efficiency of the US liver allocation system through region design. *Management Science*, 56(12):2111-2122.
- Kreke J, Schaefer AJ, Angus DC, Bryce CL, Roberts MS (2002) Incorporating biology into discrete event simulation models of organ allocation. *In Proceedings of the Winter Simulation Conference*, 1:532-536.

- Kyota F, Seigo N (2016) Size mismatch in liver transplantation. *Journal of Hepato-Biliary-Pancreatic Sciences*, 23(8):457-466.
- Lai JC, Terrault NA, Vittinghoff E, Biggins SW (2010) Height contributes to the gender difference in waitlist mortality under the MELD-based liver allocation system. *American Journal of Transplantation*, 10(12):2658-2664.
- Marvin MR, Ferguson N, Cannon RM, Jones CM, Brock GN (2015) MELD-EQ: An alternative Model for End-Stage Liver Disease score for patients with hepatocellular carcinoma. *Liver Transplantation*, 21(5):612-22.
- Massie AB, Caffo B, Gentry SE, Hall EC, Axelrod DA, Lentine KL, Schnitzler MA, Gheorghian A, Salvalaggio PR, Segev DL (2011) MELD exceptions and rates of waiting list outcomes. *American Journal of Transplantation*, 11(11):2362-2371.
- Pritsker AA, Martin DL, Reust JS, Wagner MA, Daily OP, Harper AM, Edwards EB, Bennett LE, Wilson JR, Kuhl ME, Roberts JP (1995) Organ transplantation policy evaluation. *In Proceedings of the 27th Conference on Winter Simulation*, 1314-1323.
- Reddy MS, Varghese J, Venkataraman J, Rela M (2013) Matching donor to recipient in liver transplantation: Relevance in clinical practice. *World Journal of Hepatology*, 5(11):603.
- Rickert, C. G., Z. Leung, M. Akan, J. F. Markmann, S. Tayur, H. Zhao, H. Yeh (2019a) "Stratifying HCC Patients for Liver Transplantation. REACH: Risk of Exceeding Allocation Criteria for HCC" *American Journal of Transplantation* , Vol. 19, Issue S1. p.13.
- Rickert C, Akan M, Leung Z, Markmann JF, Tayur S, Zhao H, Yeh H. (2019b) DOME: A New Strategy for Prioritizing Hepatocellular Carcinoma Patients on the Liver Transplant Waitlist [abstract]. *Am J Transplant*; 19 (suppl 3).
- Rickert C., Zhao H., Leung Z., Akan M., Markmann J., Tayur S., Yeh H. (2020) MY-ATLAS: A Novel Simulation Algorithm For Liver Transplant Allocation. *Am J Transplant*. 20(suppl 3).
- Righter R (1989) A resource allocation problem in a random environment. *Operations Research*, 37(2):329-338.
- Ruth RJ, Wyszewianski L, Herline G (1985) Kidney transplantation: A simulation model for examining demand and supply. *Management Science*, 31(5):515-526.
- Said, A, S. Erenay, M. Akan, B. Ata, O. Alagoz. Optimizing Liver Allocation Policy: 732. *Hepatology*. 50():p 647A-648A, October 2009.

- Sandıkçı B, Maillart LM, Schaefer AJ, Alagoz O, Roberts MS (2008) Estimating the patient's price of privacy in liver transplantation. *Operations Research*, 56(6):1393-1410.
- Sandıkçı B, Tunç S, Tanrıover B (2019). A new simulation model for kidney transplantation in the United States. *In 2019 Winter Simulation Conference*, 1079-1090.
- Shechter SM, Bryce CL, Alagoz O, Kreke JE, Stahl JE, Schaefer AJ, Angus DC, Roberts MS (2005) A clinically based discrete-event simulation of end-stage liver disease and the organ allocation process. *Medical Decision Making*, 25(2):199-209.
- SRTR (2019) Liver Simulated Allocation Model (LSAM) 2019 User's Guide. <https://www.srtr.org/media/1361/LSAM-2019-User-Guide.pdf>. Information and data accessed on Aug 30, 2022.
- Su X, Zenios S (2004) Patient choice in kidney allocation: The role of the queueing discipline. *Manufacturing & Service Operations Management*, 6(4):280-301.
- Su X, Zenios S (2005) Patient choice in kidney allocation: A sequential stochastic assignment model. *Operations Research*, 53(3):443-455.
- Su X, Zenios S (2006) Recipient choice can address the efficiency-equity trade-off in kidney transplantation: A mechanism design model. *Management science*, 52(11):1647-1660.
- Tang Y, Scheller-Wolf AA, Tayur SR (2021) Multi-Armed Bandits with Endogenous Learning and Queueing: An Application to Split Liver Transplantation. *Available at SSRN*, <https://ssrn.com/abstract=3855206>.
- Toso C, Dupuis-Lozeron E, Majno P, Berney T, Kneteman NM, Perneger T, Morel P, Mentha G, Combescure C (2012) A model for dropout assessment of candidates with or without hepatocellular carcinoma on a common liver transplant waiting list. *Hepatology*, 56:149-156.
- UNOS (2010) Ethical Principles in the Allocation of Human Organs. <https://optn.transplant.hrsa.gov/resources/ethics/ethical-principles-in-the-allocation-of-human-organs/>. Information and data accessed on Nov 17, 2021.
- UNOS (2021) Transplant trends. <https://unos.org/data/transplant-trends/>. Information and data accessed on Nov 17, 2021.
- Vitale A, Volk ML, De Feo TM, Burra P, Frigo AC, Morales RR, De Carlis L, Belli L, Colledan M, Fagioli S, Rossi G (2014) A method for establishing allocation equity among patients with

and without hepatocellular carcinoma on a common liver transplant waiting list. *Journal of Hepatology*, 60(2):290-7.

Zenios SA, Chertow GM, Wein LM (2000) Dynamic allocation of kidneys to candidates on the transplant waiting list. *Operations Research*, 48(4):549-569.

Appendix A. Estimation of ESLD patients' 90-day mortality risk

The logistic regression coefficients used for predicting 90-day mortality risk of ESLD patients can be seen in Table 6.

Table 6: Logistic regression coefficients for predicting 90-day mortality risk

	Coefficient	Standard Error	z value	$P(> z)$
Intercept	-6.817	0.024	-280.1	$< 10^{-6}$
Laboratory MELD	0.237	0.001	221.5	$< 10^{-6}$

Appendix B. Proofs

Derivation of the dual problem (D).

We follow the road map provided by Rockafellar (1970) to derive the dual problem of control associated with (P). In particular, we first append the penalty expressions corresponding to the organ availability restrictions on allocations in the objective function by defining the convex, extended real valued integrand L and the convex functional l . Next, we compute the conjugate convex functions associated with L and l so as to define the dual integrand M and the dual functional m . The dual problem of control is defined using M and m .

We can write our convex integrand L on $[0, T] \times \mathbb{R}^{IJ} \times \mathbb{R}^{IJ} \times \mathbb{R}^{IJ} \times \mathbb{R}^{IJ}$ as follows (for the sake of notation, t is dropped for time dependent variables):

$$\begin{aligned}
 L(t, x, \dot{x}, w, \dot{w}) &= (e \cdot d) \cdot x + \chi_{\mathbb{R}_+^{IJ}}(x) + \chi_{\mathbb{R}_+^{IJ}}(w) + \sum_{k=1}^K \chi_{\mathbb{R}_+^{IJ}}(u^k) + \sum_{k=1}^K \chi_{\mathbb{R}_-}(e \cdot u^k - \mu_k(t)) \\
 &\quad + \sum_{(i,k) \in INF} \chi_{\mathbb{R}_-}(e \cdot u_i^k - \epsilon)
 \end{aligned}$$

if $\dot{x}(t) = \lambda(t) - \sum_{k=1}^K P^k u^k(t) - (d + \beta - \gamma)x(t)$ and $\dot{w}(t) = u(t)$, otherwise $L(t, x, \dot{x}, w, \dot{w}) = \infty$.

This way, we append the hard constraints of (P) as penalty expressions to the objective function.

The expressions $\chi_{\mathbb{R}_+^{IJ}}(x)$ and $\chi_{\mathbb{R}_+^{IJ}}(w)$ ensure the non-negativity of the state variables x and w , and the expression $\sum_{k=1}^K \chi_{\mathbb{R}_+^{IJ}}(u^k)$ ensures the non-negativity of the control variable u . The constraint related to the allocation of organs not exceeding the supply is expressed by the penalty term $\sum_{k=1}^K \chi_{\mathbb{R}_-}(e \cdot u^k - \mu_k(t))$ and the infeasible allocations is expressed by $\sum_{(i,k) \in INF} \chi_{\mathbb{R}_-}(e \cdot u_i^k - \epsilon)$.

We note that the infeasible allocations are restricted within ϵ . The system dynamics equations are incorporated in L by requiring $\dot{x}(t)$ to be equal to $\lambda(t) - \sum_{k=1}^K P^k u^k(t) - (d + \beta - \gamma)x(t)$ and $\dot{w}(t)$

to be equal to $u(t)$.

Next, we define the functional l on $\mathbb{R}^{IJ} \times \mathbb{R}^{IJ} \times \mathbb{R}^{IJ}$ taking values on $\mathbb{R} \cup \{\infty\}$ for the initial state of the problem and terminal conditions. Initially, there are $x_{ij}(0)$ patients in class ij and $w(0)$ is equal to 0 because we have not allocated any organs yet. As the terminal condition, $x(T)$ is not restricted because we minimize pre-transplant mortality on $[0, T]$ and we have $e \cdot w(T) = \lambda T / \rho$ to ensure that all patient classes have an equal likelihood of receiving an organ transplant. The functional l is defined as $l(x_0, w_0, w_T) = l_0(x_0, w_0) + l_T(w_T)$ where $l_0(x_0, w_0) = \chi_{\{(x(0), 0)\}}(x_0, w_0)$ and $l_T(w_T) = \chi_{\{\lambda T / \rho\}}(w_T)$. The functional l_0 and l_T dictate the initial and terminal state conditions, respectively. As a result, the primal problem (P) becomes a problem of minimizing

$$\int_0^T L(t, x(t), \dot{x}(t), w(t), \dot{w}(t)) dt + l(x_0, w_0, w_T).$$

In our next step, we compute the conjugates to the functions L and l . Let L^* denote the conjugate to L . To be specific,

$$L^*(t, s, p, r, q) = \sup_{z \in \mathbb{R}^{IJ}, y \in \mathbb{R}^{IJ}, v \in \mathbb{R}^{IJ}, m \in \mathbb{R}^{IJ}} \{z \cdot s + y \cdot p + v \cdot r + m \cdot q - L(t, z, y, v, m)\}$$

for $s, p, r, q \in \mathbb{R}^{IJ}$. We can express L^* more explicitly as follows. Note that $L(t, z, y, v, k) < \infty$ only if $z \geq 0$, $v \geq 0$ and there exists some $u^k \in \mathbb{R}_+^{IJ}$ such that $y = \lambda(t) - \sum_{k=1}^K P^k u^k - (d + \beta - \gamma)z$, $m^k = u^k$, $e \cdot u^k \leq \mu_k(t)$, $u_i^k \leq \epsilon$ for $(i, k) \in INF$ and $u^k \geq 0$ for $k \in \mathcal{K}$. For $s, p, r, q \in \mathbb{R}^{IJ}$, we write L^* as

$$L^*(t, s, p, r, q) = \sup_{z \in \mathbb{R}_+^{IJ}, u(t) \in \Phi(t), v \in \mathbb{R}^{IJ}} \left\{ z \cdot s + p \cdot \left(\lambda(t) - \sum_{k=1}^K P^k u^k - (d + \beta - \gamma)z \right) + v \cdot r \right. \\ \left. + q \cdot u^k - (e \cdot d) \cdot z \right\}$$

by replacing y with $\lambda(t) - \sum_{k=1}^K P^k u^k - (d + \beta - \gamma)z$, m^k with u^k for feasible u^k and noting that $L(t, z, y, v, k) = (e \cdot d) \cdot z$. We rearrange the terms as follows

$$L^*(t, s, p, r, q) = \sup_{z \in \mathbb{R}_+^{IJ}} \{z \cdot (s - p(d + \beta - \gamma) - e \cdot d)\} + p \cdot \lambda(t) + \sup_{v \in \mathbb{R}^{IJ}} \{v \cdot r\} \\ + \sup_{u(t) \in \Phi(t)} \sum_{k=1}^K \{-p \cdot P^k u^k + q \cdot u^k\}$$

because we can take the supremum for z , v and u^k separately for each k . We have $\sup_{z \in \mathbb{R}_+^{IJ}} \{z \cdot (s -$

$p(d + \beta - \gamma) - e \cdot d\} = \chi_{\mathbb{R}^I} \{s - p(d + \beta - \gamma) - e \cdot d\}$ since $\sup_{z \in \mathbb{R}^I} \{z \cdot (s - p(d + \beta - \gamma) - e \cdot d)\}$ becomes ∞ if $(s - p(d + \beta - \gamma) - e \cdot d)_{ij} > 0$ for $i \in \mathcal{I}$ and $j \in \mathcal{J}$. Also, we obtain $\sup_{u(t) \in \Phi(t)} \sum_{k=1}^K \{-p \cdot P^k u^k + q \cdot u^k\} = \inf_{u(t) \in \Phi(t)} \sum_{k=1}^K \{(p \cdot P^k - q)u^k\}$. Therefore, L^* can be written as follows

$$L^*(t, s, p, r, q) = \chi_{\mathbb{R}^I} \{s - p(d + \beta - \gamma) - e \cdot d\} + p \cdot \lambda(t) + \sup_{v \in \mathbb{R}^I} \{v \cdot r\} + \inf_{u(t) \in \Phi(t)} \sum_{k=1}^K \{(p \cdot P^k - q)u^k\}.$$

Using the conjugate L^* of the primal integrand L , we calculate the dual integrand M . For $t \in [0, T]$ and $s, p, r, q \in \mathbb{R}^I$, the dual integrand M is given by $M(t, p, s, q, r) = L^*(t, s, p, r, q)$. That is, for $t \in [0, T]$, we have

$$\begin{aligned} M(t, y(t), \dot{y}(t), z(t), \dot{z}(t)) &= L^*(t, \dot{y}(t), y(t), \dot{z}(t), z(t)) \\ &= \chi_{\mathbb{R}^I} \{\dot{y}(t) - y(t)(d + \beta - \gamma) - e \cdot d\} + y(t) \cdot \lambda(t) + \sup_{v \in \mathbb{R}^I} \{v \cdot \dot{z}(t)\} \\ &\quad + \inf_{u(t) \in \Phi(t)} \sum_{k=1}^K \{(y(t) \cdot P^k - z(t))u^k\}, \end{aligned}$$

where $\chi_{\mathbb{R}^I} \{\dot{y}(t) - y(t)(d + \beta - \gamma) - e \cdot d\}$ ensures that $\dot{y}(t) \leq y(t)(d + \beta - \gamma) + d$ for $t \in [0, T]$. Finally, we need to derive the terminal conditions associated with the dual problem. For this, we define the functional m on $\mathbb{R}^I \times \mathbb{R}^I \times \mathbb{R}^I$ as follows:

$$m(y_0, z_0, z_T) = l_0^*(y_0, z_0) + l_T^*(-z_T)$$

where l_0^* and l_T^* are the conjugates of l_0 and l_T . We calculate l_0^* as follows: $l_0^*(y_0, z_0) = \sup_{x, w} \{y \cdot x + z \cdot w - l_0(x, w)\} = \sup_{x \in \{x(0)\}, w=0} \{y \cdot x\} = x(0) \cdot y$. Similarly, $l_T^*(-z_T) = \sup_w \{w \cdot z\} = \sup_{w=\lambda T/\rho} \{-w \cdot z\} = -z \lambda T/\rho$. The dual problem of control is to minimize

$$\int_0^T M(t, y(t), \dot{y}(t), z(t), \dot{z}(t)) dt + m(y_0, z_0, z_T)$$

that is equivalent to minimizing

$$\int_0^T [y(t)\lambda(t) + f(t, y(t), z(t))]dt + x(0) \cdot y(0) - \frac{z(T)\lambda T}{\rho}$$

subject to

$$\begin{aligned} y(t) &= y(0) + \int_0^t \dot{y}(s)ds \\ z(t) &= \int_0^t \dot{z}(s)ds \\ \dot{z}(t) &= 0 \\ \dot{y}(t) &\leq y(t)(d + \beta - \gamma) + d \end{aligned} \tag{D}$$

where $f(t, y(t), z(t)) = \inf \sum_{k=1}^K \{(y(t) \cdot P^k - z(t))u^k : u(t) \in \Phi(t)\}$. ■

Proof of Theorem 1. To show that the objective function values of the primal problem (P) and the dual problem (D) are equal to each other by using Theorem 4 of Rockafellar (1970), we need to show that the primal problem (P) is feasible and bounded. It is bounded because $e \cdot u^k(t) \leq \mu_k(t)$ for $k \in \mathcal{K}$ and $t \geq 0$. Given that the primal problem is bounded, $\dot{z}(t) = 0$ to ensure that the dual problem is bounded as well. To show that there is a feasible u satisfying the constraints of P, we need an additional assumption on the likelihood of transplant constraint. The average likelihood of transplantation, $1/\rho$, must be small enough so that there exists u such that $e \cdot u^k(t) \leq \mu_k(t)$, $w(t) = \int_0^t u(\tau)d\tau$ and $w(T) = \lambda T/\rho$. With this additional assumption, we conclude that the primal problem (P) is also feasible ensuring that the objective function values of (P) and (D) are equal to each other.

We need to derive the coextremality conditions for the primal - dual problem pair to complete the proof. By Theorem 5 of Rockafellar (1970), let u be a feasible organ allocation for (P) with the corresponding state trajectories x and w , and let y and z be a feasible control for (D), the control u is optimal for (P) and y and z are optimal for (D), if and only if they satisfy the following coextremality conditions:

$$\begin{aligned} (y(0), z(0), -z(T)) &\in \partial l(x(0), w(0), w(T)) \text{ and} \\ (\dot{y}(t), y(t), \dot{z}(t), z(t)) &\in \partial L(t, x(t), \dot{x}(t), w(t), \dot{w}(t)) \text{ for almost every } t \in (0, T) \end{aligned}$$

where ∂L and ∂l are the subgradients of the convex integrand L and the functional l , defined above. First, we calculate the subgradient of L from its epigraphical normals. For $h : \mathbb{R}^n \rightarrow [-\infty, +\infty]$ and any point \bar{x} at which h is finite, we have $\partial h(\bar{x}) = \{v : (v, -1) \in N_{\text{epi } h}(\bar{x}, h(\bar{x}))\}$ where $\text{epi } h$

denotes the epigraph of h defined as $\text{epi } h := \{(x, \gamma) \in \mathbb{R}^n \times \mathbb{R} : \gamma \geq h(x)\}$, and $N_{\text{epi } h}(\bar{x}, h(\bar{x}))$ is the set of vectors to the set $\text{epi } h$ at $(\bar{x}, h(\bar{x}))$ in the general sense as in Definition 6.3 of Rockafellar & Wets (1997). For $t \in [0, T]$, the epigraph of the integrand L is defined as follows: $\text{epi } L(t)$ consists of points $(x, \dot{x}, w, \dot{w}, \gamma) \in \mathbb{R}^{4IJ+1}$ such that

$$\begin{aligned} \dot{x} &= \lambda(t) - \sum_{k=1}^K P^k u^k - (d + \beta - \gamma)x, \quad \dot{w}^k = u^k, \quad x \geq 0, \quad w \geq 0, \quad \gamma \geq (e \cdot d) \cdot x, \\ e \cdot u^k(t), u^k &\geq 0 \text{ for } k \in \mathcal{K}, u_i^k(t) \leq \epsilon \text{ for } (i, k) \in INF, \end{aligned}$$

since the points $(x, \dot{x}, w, \dot{w}) \in \mathbb{R}^{4IJ}$ where $L(t, x, \dot{x}, w, \dot{w}) = \infty$ are such that the vertical line $(x, \dot{x}, w, \dot{w}) \times \mathbb{R}$ misses $\text{epi } L(t)$. Then, we can write

$$\partial L(t, \bar{x}, \bar{\dot{x}}, \bar{w}, \bar{\dot{w}}) = \left\{ (v^1, v^2, v^3, v^4) \in \mathbb{R}^{4IJ} : (v^1, v^2, v^3, v^4, -1) \in N_{\text{epi } L(t)}(\bar{x}, \bar{\dot{x}}, \bar{w}, \bar{\dot{w}}, L(t, \bar{x}, \bar{\dot{x}}, \bar{w}, \bar{\dot{w}})) \right\}.$$

First, note that for $t \in [0, T]$, $\text{epi } L(t)$ is a convex set and the point $(\bar{x}, \bar{\dot{x}}, \bar{w}, \bar{\dot{w}}, L(t, \bar{x}, \bar{\dot{x}}, \bar{w}, \bar{\dot{w}}))$ is an element of $\text{epi } L(t)$ for $(\bar{x}, \bar{\dot{x}}, \bar{w}, \bar{\dot{w}}) \in \mathbb{R}^{4IJ}$. Let \mathbf{v} denote an arbitrary element of \mathbb{R}^{4IJ+1} where the first IJ components of \mathbf{v} is denoted as v^1 , the subsequent IJ components by v^2, v^3 and v^4 , and the last component by v^γ . That is, $\mathbf{v} = [v^1, v^2, v^3, v^4]^T$ where $v^1, v^2, v^3, v^4 \in \mathbb{R}^{IJ}$ and $v^\gamma \in \mathbb{R}$. Then, we use Theorem 6.9 of Rockafellar & Wets (1997) which gives

$$\begin{aligned} &N_{\text{epi } L(t)}(\bar{x}, \bar{\dot{x}}, \bar{w}, \bar{\dot{w}}, L(t, \bar{x}, \bar{\dot{x}}, \bar{w}, \bar{\dot{w}})) \\ &= \left\{ \mathbf{v} \in \mathbb{R}^{4IJ+1} : \left[(x, \dot{x}, w, \dot{w}, \gamma) - (\bar{x}, \bar{\dot{x}}, \bar{w}, \bar{\dot{w}}, L(t, \bar{x}, \bar{\dot{x}}, \bar{w}, \bar{\dot{w}})) \right] \cdot \mathbf{v} \leq 0, \forall (x, \dot{x}, w, \dot{w}, \gamma) \in \text{epi } L(t) \right\}. \end{aligned} \tag{10}$$

We next establish the following properties of $N_{\text{epi } L(t)}(\bar{x}, \bar{\dot{x}}, \bar{w}, \bar{\dot{w}}, L(t, \bar{x}, \bar{\dot{x}}, \bar{w}, \bar{\dot{w}}))$ for $t \in [0, T]$ which will assist us in finding the subgradients of L .

Property 1. For $t \in [0, T]$, if $\mathbf{v} = (v^1, v^2, v^3, v^4, v^\gamma)^T \in N_{\text{epi } L(t)}(\bar{x}, \bar{\dot{x}}, \bar{w}, \bar{\dot{w}}, L(t, \bar{x}, \bar{\dot{x}}, \bar{w}, \bar{\dot{w}}))$, then $v^1 \leq v^2(d + \beta - \gamma) - v^\gamma d$. Moreover, $v_{ij}^1 = -v^\gamma d_{ij} + [v^2(d + \beta - \gamma)]_{ij}$ when $\bar{x}_{ij} > 0$.

To verify Property 1, we first show that any $\mathbf{v} = (v^1, v^2, v^3, v^4, v^\gamma)^T$ such that $v_{ij}^1 > -v^\gamma d_{ij} + [v^2(d + \beta - \gamma)]_{ij}$ for some ij cannot be in $N_{\text{epi } L(t)}(\bar{x}, \bar{\dot{x}}, \bar{w}, \bar{\dot{w}}, L(t, \bar{x}, \bar{\dot{x}}, \bar{w}, \bar{\dot{w}}))$. Suppose not. Then, we could find an element $(\tilde{x}, \tilde{\dot{x}}, \tilde{w}, \tilde{\dot{w}}, \tilde{\gamma})$ of $\text{epi } L(t)$ such that it is equal to $(\bar{x}, \bar{\dot{x}}, \bar{w}, \bar{\dot{w}}, L(t, \bar{x}, \bar{\dot{x}}, \bar{w}, \bar{\dot{w}}) + d_{ij}(\tilde{x}_{ij} - \bar{x}_{ij}))$ except for $\tilde{x}_{ij} > \bar{x}_{ij}$ and $\tilde{\dot{x}} = \lambda(t) - \sum_{k=1}^K P^k u^k - (d + \beta - \gamma)\tilde{x}$. However, in that

case, we obtain

$$\begin{aligned}
\left[(\tilde{x}, \tilde{\dot{x}}, \tilde{w}, \tilde{\dot{w}}, \tilde{\gamma}) - (\bar{x}, \bar{\dot{x}}, \bar{w}, \bar{\dot{w}}, L(t, \bar{x}, \bar{\dot{x}}, \bar{w}, \bar{\dot{w}})) \right] \cdot \mathbf{v} &= v_{ij}^1(\tilde{x}_{ij} - \bar{x}_{ij}) + v^2 \cdot (\tilde{\dot{x}} - \bar{\dot{x}}) + v^\gamma d_{ij}(\tilde{x}_{ij} - \bar{x}_{ij}) \\
&= (\tilde{x}_{ij} - \bar{x}_{ij})(v_{ij}^1 + v^\gamma d_{ij}) + v^2(d + \beta - \gamma)(\tilde{\dot{x}} - \bar{\dot{x}}) \\
&= \left(v_{ij}^1 + v^\gamma d_{ij} - [v^2(d + \beta - \gamma)]_{ij} \right) (\tilde{x}_{ij} - \bar{x}_{ij}) \\
&> 0,
\end{aligned}$$

contradicting that $(v^1, v^2, v^3, v^4, v^\gamma)^T \in N_{\text{epi } L(t)}(\bar{x}, \bar{\dot{x}}, \bar{w}, \bar{\dot{w}}, L(t, \bar{x}, \bar{\dot{x}}, \bar{w}, \bar{\dot{w}}))$. Similarly, we can show that if $\bar{x}_{ij} > 0$, then any $\mathbf{v} = (v^1, v^2, v^3, v^4, v^\gamma)^T$ such that $v_{ij}^1 \neq -v^\gamma d_{ij} + [v^2(d + \beta - \gamma)]_{ij}$ for some ij cannot be in $N_{\text{epi } L(t)}(\bar{x}, \bar{\dot{x}}, \bar{w}, \bar{\dot{w}}, L(t, \bar{x}, \bar{\dot{x}}, \bar{w}, \bar{\dot{w}}))$. Therefore, Property 1 proves the coextremality condition that for $t \in [0, T]$, $\dot{y}(t) \leq d + y(t)(d + \beta - \gamma)$ and whenever $x_{ij}(t) > 0$, it must be that $\dot{y}_{ij}(t) = d_{ij} + [y(t)(d + \beta - \gamma)]_{ij}$.

Property 2. For $t \in [0, T]$, if $\mathbf{v} = (v^1, v^2, v^3, v^4, v^\gamma)^T \in N_{\text{epi } L(t)}(\bar{x}, \bar{\dot{x}}, \bar{w}, \bar{\dot{w}}, L(t, \bar{x}, \bar{\dot{x}}, \bar{w}, \bar{\dot{w}}))$, then $v^3 \leq 0$. Similar to Property 1, we show that any $\mathbf{v} = (v^1, v^2, v^3, v^4, v^\gamma)^T$ such that $v_{ij}^3 > 0$ for some ij cannot be in $N_{\text{epi } L(t)}(\bar{x}, \bar{\dot{x}}, \bar{w}, \bar{\dot{w}}, L(t, \bar{x}, \bar{\dot{x}}, \bar{w}, \bar{\dot{w}}))$. Suppose not. Then, we could find an element $(\tilde{x}, \tilde{\dot{x}}, \tilde{w}, \tilde{\dot{w}}, \tilde{\gamma})$ of $\text{epi } L(t)$ such that it is equal to $(\bar{x}, \bar{\dot{x}}, \bar{w}, \bar{\dot{w}}, L(t, \bar{x}, \bar{\dot{x}}, \bar{w}, \bar{\dot{w}}))$ except for $\tilde{w}_{ij} > \bar{w}_{ij}$. In that case, we obtain

$$\begin{aligned}
\left[(\tilde{x}, \tilde{\dot{x}}, \tilde{w}, \tilde{\dot{w}}, \tilde{\gamma}) - (\bar{x}, \bar{\dot{x}}, \bar{w}, \bar{\dot{w}}, L(t, \bar{x}, \bar{\dot{x}}, \bar{w}, \bar{\dot{w}})) \right] \cdot \mathbf{v} &= v_{ij}^3(\tilde{w}_{ij} - \bar{w}_{ij}) \\
&> 0,
\end{aligned}$$

contradicting that $(v^1, v^2, v^3, v^4, v^\gamma)^T \in N_{\text{epi } L(t)}(\bar{x}, \bar{\dot{x}}, \bar{w}, \bar{\dot{w}}, L(t, \bar{x}, \bar{\dot{x}}, \bar{w}, \bar{\dot{w}}))$. Therefore, Property 2 along with the fact that the primal problem is bounded proves the coextremality condition that for $t \in [0, T]$, $\dot{z}(t) = 0$.

Property 3. For $t \in [0, T]$ and $k \in \mathcal{K}$, if $\bar{\dot{x}} = \lambda(t) - \sum_{k=1}^K P^k \bar{u}^k - (d + \beta - \gamma)\bar{x}$ and $\bar{\dot{w}} = \bar{u}$ for \bar{u}^k such that $\bar{u}^k \geq 0$, $e \cdot \bar{u}^k \leq \mu_k(t)$, $\bar{u}_i^k \leq \epsilon$ for $(i, k) \in \text{INF}$ and $\mathbf{v} = (v^1, v^2, v^3, v^4, v^\gamma) \in N_{\text{epi } L(t)}(\bar{x}, \bar{\dot{x}}, \bar{w}, \bar{\dot{w}}, L(t, \bar{x}, \bar{\dot{x}}, \bar{w}, \bar{\dot{w}}))$, then, $\bar{u}^k \in \arg \min_{z \in \Phi(t)} \left\{ (P^k \cdot v^2 - v^4) \cdot z^k \right\}$.

To establish Property 3, we first recall that for any $(x, \dot{x}, w, \dot{w}, \gamma) \in \text{epi } L(t)$, there exists some $u^k \in \mathbb{R}^{IJ}$ for $k \in \mathcal{K}$ such that

$$\dot{x} = \lambda(t) - \sum_{k=1}^K P^k u^k - (d + \beta - \gamma)x, \quad \dot{w}^k = u^k, \quad x \geq 0, \quad w \geq 0, \quad u^k(t) \in \Phi(t), \quad \text{and } \gamma \geq (e \cdot d) \cdot x$$

For an arbitrary $k' \in \mathcal{K}$, consider now an element $(\bar{x}, \bar{\dot{x}}, \bar{w}, \bar{\dot{w}}, (e \cdot d) \cdot x) \in \text{epi } L(t)$ where $\bar{\dot{x}} = \lambda(t) - (d + \beta - \gamma)\bar{x} - \sum_{k \neq k'}^K P^k \bar{u}^k - P^{k'} u^{k'}$, $\bar{\dot{w}}^k = \bar{u}^k$ for $k \neq k'$ and $\bar{\dot{w}}^{k'} = u^{k'}$. Then, the following

holds for $\mathbf{v} = (v^1, v^2, v^3, v^4, v^\gamma) \in N_{\text{epi } L(t)}(\bar{x}, \bar{\dot{x}}, \bar{w}, \bar{\dot{w}}, L(t, \bar{x}, \bar{\dot{x}}, \bar{w}, \bar{\dot{w}}))$:

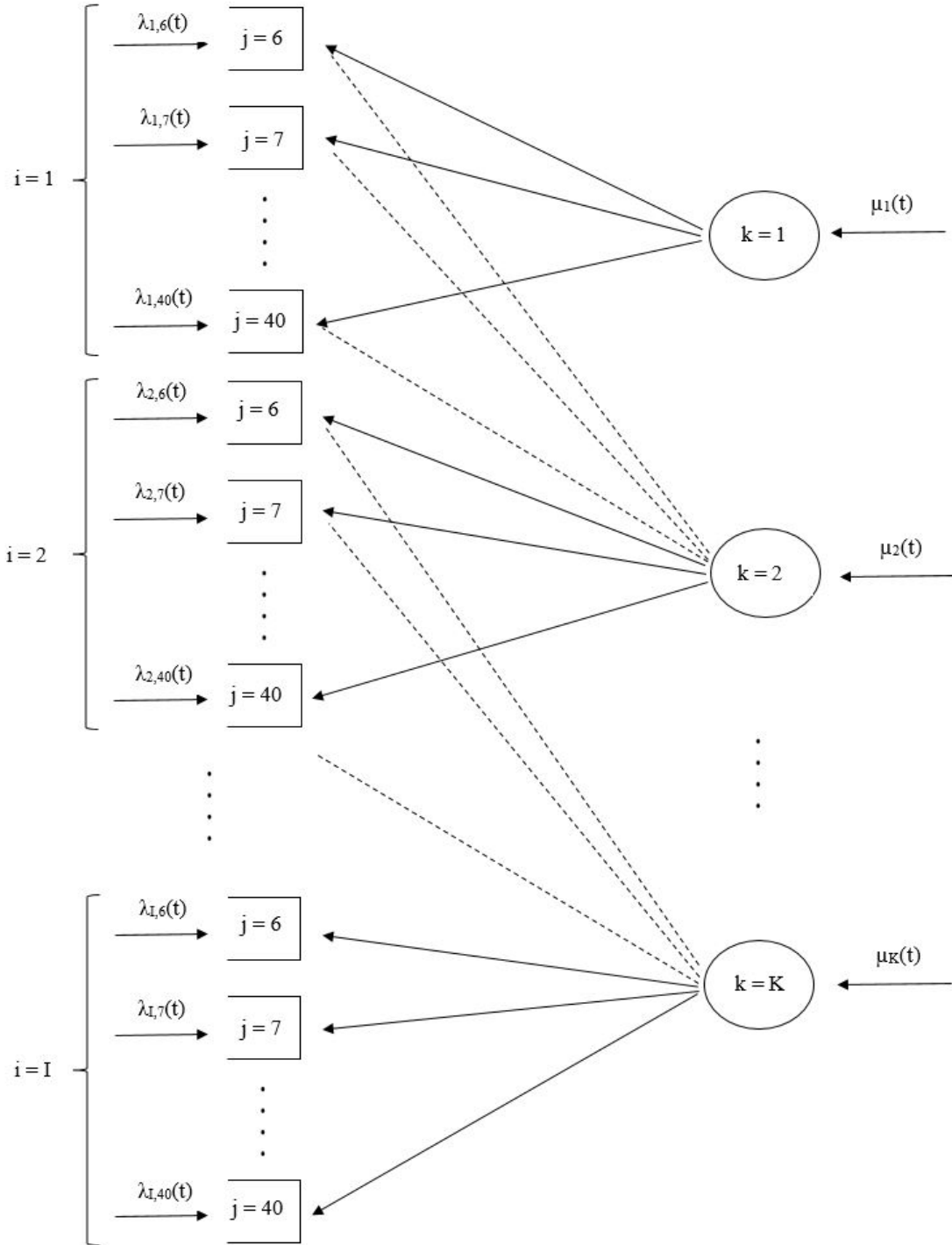
$$\begin{aligned}
& \left[\left(\bar{x}, \dot{x}, \bar{w}, \dot{w}, (e \cdot d) \cdot x \right) - \left(\bar{x}, \bar{\dot{x}}, \bar{w}, \bar{\dot{w}}, L(\bar{x}, \bar{\dot{x}}, \bar{w}, \bar{\dot{w}}) \right) \right] \cdot \mathbf{v} \\
&= v^1 \cdot (\bar{x} - \bar{x}) + v^2 \cdot (\dot{x} - \bar{\dot{x}}) + v^3 \cdot (\bar{w} - \bar{w}) + v^4 \cdot (\dot{w} - \bar{\dot{w}}) + v^\gamma \cdot (-(e \cdot d) \cdot \bar{x} + (e \cdot d) \cdot \bar{x}) \\
&= v^2 \cdot (-P^{k'} u^{k'} + P^{k'} \bar{u}^{k'}) + v^4 \cdot (u^{k'} - \bar{u}^{k'}) \\
&= (P^{k'} \cdot v^2 - v^4)(\bar{u}^{k'} - u^{k'}).
\end{aligned}$$

Then, we have $(P^{k'} \cdot v^2 - v^4)(\bar{u}^{k'} - u^{k'}) \leq 0$, only if $(P^{k'} \cdot v^2 - v^4)u^{k'} \geq (P^{k'} \cdot v^2 - v^4)\bar{u}^{k'}$. From (6), since $(\bar{x}, \dot{x}, \bar{w}, \dot{w}, (e \cdot d) \cdot x)$ is an element of $\text{epi } L(t)$, this proves Property 3. Recall that the subgradient of L is related to the normal cone of its epigraph as $\partial L(t, \bar{x}, \bar{\dot{x}}, \bar{w}, \bar{\dot{w}}) = \left\{ (v^1, v^2, v^3, v^4) \in \mathbb{R}^{4IJ} : (v^1, v^2, v^3, v^4, -1) \in N_{\text{epi } L(t)}(\bar{x}, \bar{\dot{x}}, \bar{w}, \bar{\dot{w}}, L(t, \bar{x}, \bar{\dot{x}}, \bar{w}, \bar{\dot{w}})) \right\}$. The coextremality conditions state that for all $t \in [0, T]$, $(\dot{y}(t), y(t), \dot{z}(t), z(t)) \in \partial L(t, x(t), \dot{x}(t), w(t), \dot{w}(t))$. That is, for $t \in [0, T]$, $(\dot{y}(t), y(t), \dot{z}(t), z(t), -1) \in N_{\text{epi } L(t)}(x(t), \dot{x}(t), w(t), \dot{w}(t), L(t, x(t), \dot{x}(t), w(t), \dot{w}(t)))$. This implies that $u^k(t) \in \arg \min_{v \in \Phi(t)} \{(y(t) \cdot P^k - z(t))v\}$, which establishes the coextremality condition. This concludes the proof of Theorem 1. ■

Appendix C. Dynamics of the Liver Allocation System

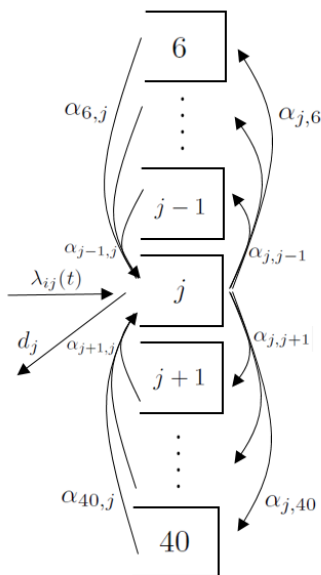
The diagram of the liver allocation system is presented in Figure 5. Figure 6 shows the dynamic changes in class ij patients' health condition that is captured by their laboratory MELD score.

Figure 5: Diagram of the Liver Allocation System



Notes. Static patient classes are denoted by $i \in \{1, 2, \dots, I\}$ and dynamic patient classes are denoted by $j \in \{6, \dots, 40\}$ corresponding to transplant candidates' laboratory MELD scores. The classes of deceased donor livers are denoted by $k \in \{1, 2, \dots, K\}$. The solid lines represent the identical donor-recipient matches and the dashed lines represent the other compatible matches.

Figure 6: Dynamics of class ij patients



Notes. $\lambda_{ij}(t)$ denotes the arrival rate of class ij patients. d_j denotes the mortality rate of patients with MELD score j . $\alpha_{j'j}$ denotes patients' health transition rate from MELD score j' to j , and $\alpha_{jj'}$ denotes patients' health transition rate from MELD score j to j' .

Appendix D. Size-Based Compatibility Analysis

As we discussed in §5, we created a compatibility matrix for each donor-recipient height class pair using the BSA analysis. The compatibility percentages can be seen in Table 7.

Table 7: Size-Based Compatibility Matrix (%)
Recipient Height (cm)

		Recipient Height (cm)				
		≤ 150 cm	151-156 cm	157-165 cm	166-175 cm	≥ 176 cm
Donor Height (cm)	≤ 150 cm	97.8	97.4	97.4	93.2	67.2
	151-156 cm	98.2	99.2	98.4	98.4	83.4
	157-165 cm	93.6	1	1	1	97.8
	166-175 cm	85.9	99.3	1	1	1
	≥ 176 cm	40.5	90.7	97.3	1	1

Table 7 shows that same height tier donor-recipient pairs are the most compatible as expected, i.e., the diagonal entries of the matrix are either or very close to one. The least compatible donor-recipient pairs are donors (recipients) with ≤ 150 cm and recipients (donors) with ≥ 176 cm. The remaining donor-recipient pairs show a high percentage of size-based compatibility ($\geq 80\%$).

BSA histograms and quantiles of each donor and recipient height tier can be found in figures below.

Figure 7: BSA Histogram of ≤ 150 cm Donors

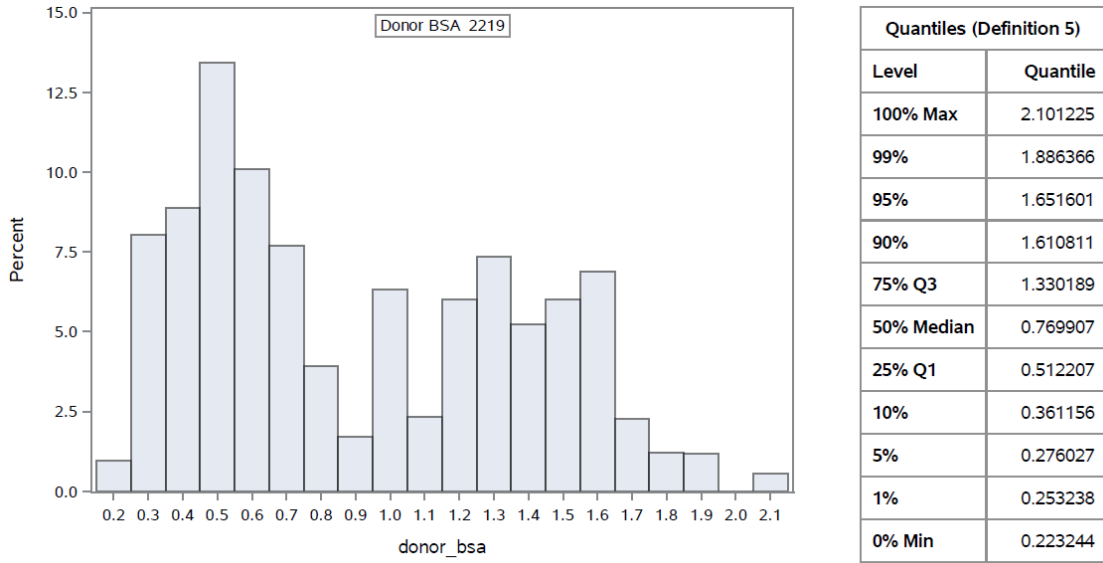


Figure 8: BSA Histogram of 151-156 cm Donors

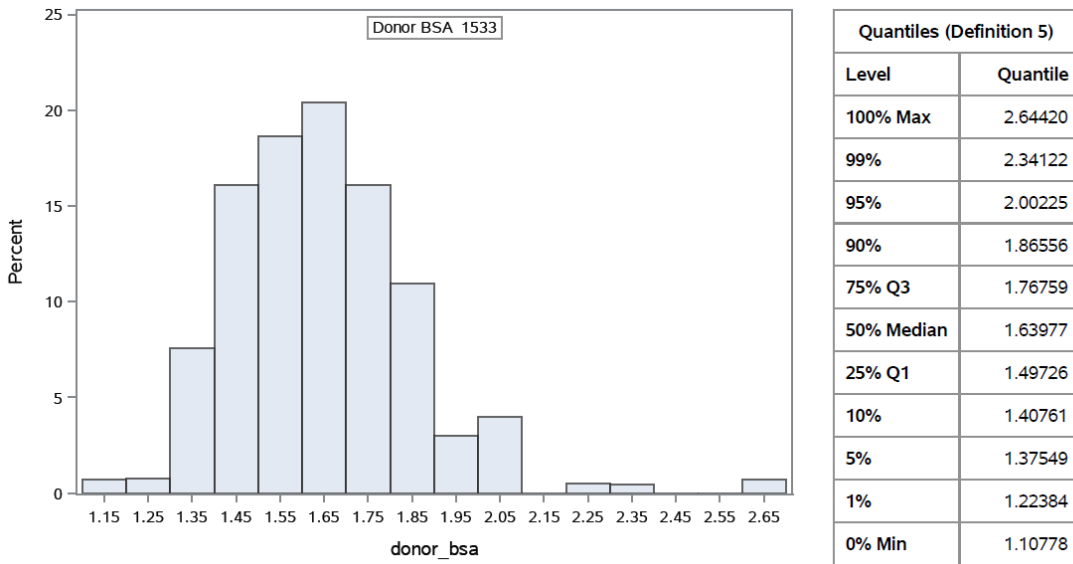
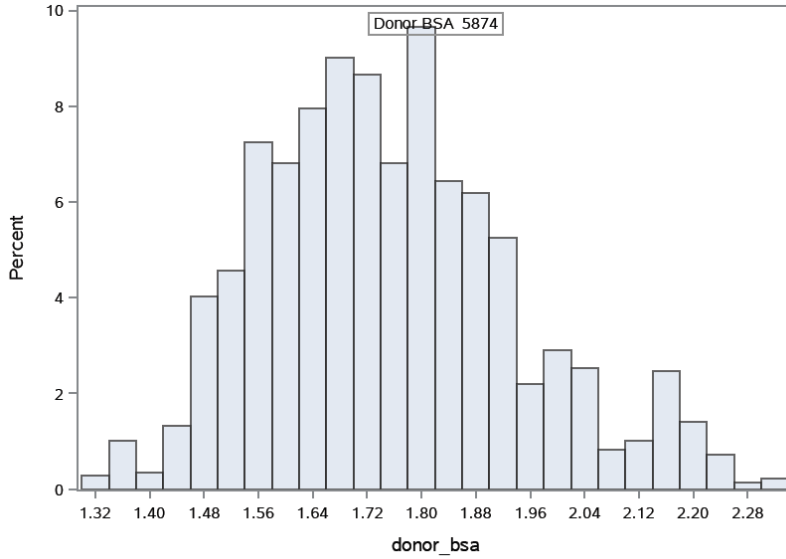
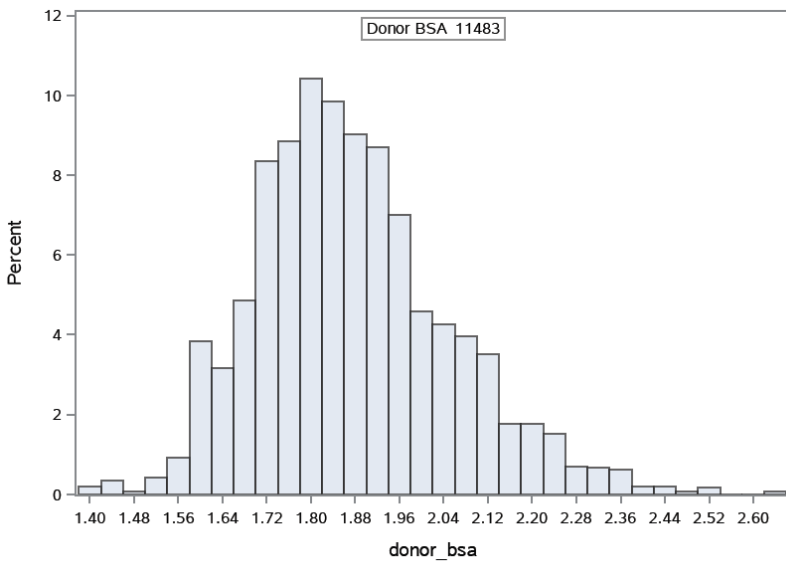


Figure 9: BSA Histogram of 157-165 cm Donors



Quantiles (Definition 5)	
Level	Quantile
100% Max	2.33223
99%	2.22062
95%	2.12978
90%	2.01279
75% Q3	1.86448
50% Median	1.73205
25% Q1	1.61262
10%	1.52024
5%	1.47940
1%	1.37796
0% Min	1.30419

Figure 10: BSA Histogram of 166-175 cm Donors



Quantiles (Definition 5)	
Level	Quantile
100% Max	2.64543
99%	2.35807
95%	2.19583
90%	2.10841
75% Q3	1.97668
50% Median	1.85206
25% Q1	1.75035
10%	1.67035
5%	1.61266
1%	1.53948
0% Min	1.39462

Figure 11: BSA Histogram of ≥ 176 cm Donors

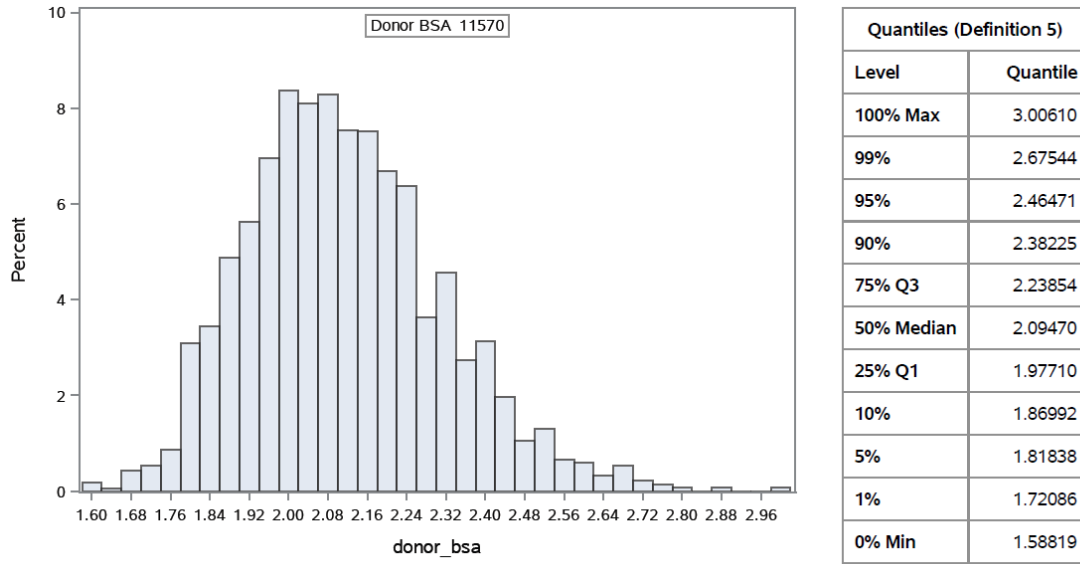


Figure 12: BSA Histogram of ≤ 150 cm Patients

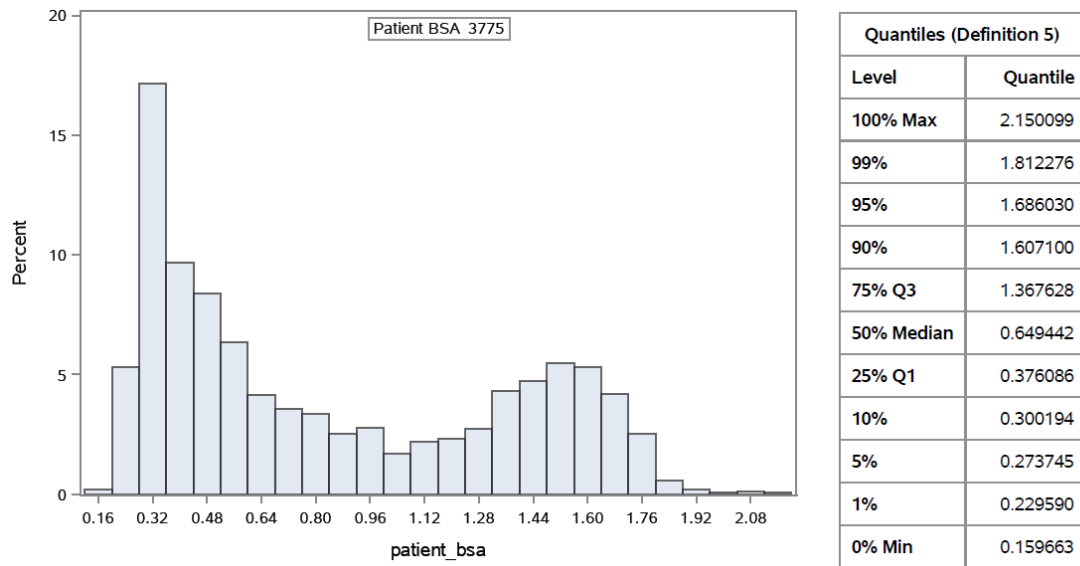
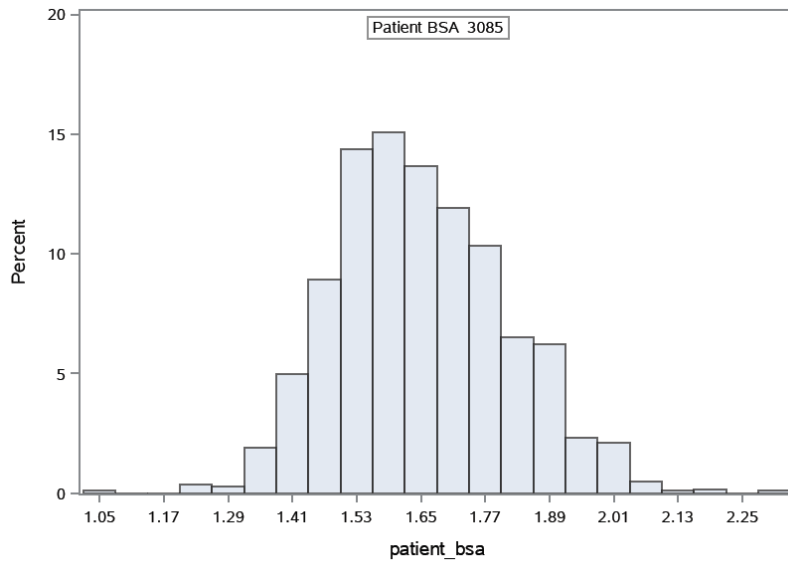
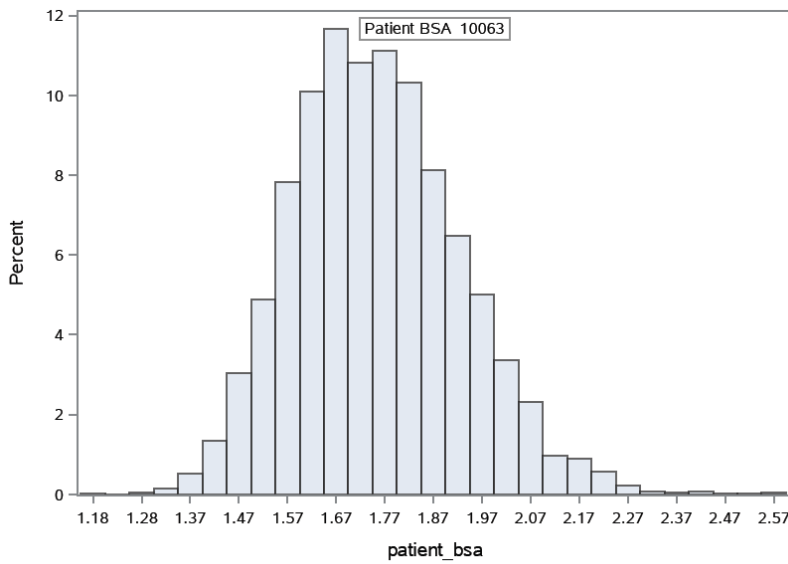


Figure 13: BSA Histogram of 151-156 cm Patients



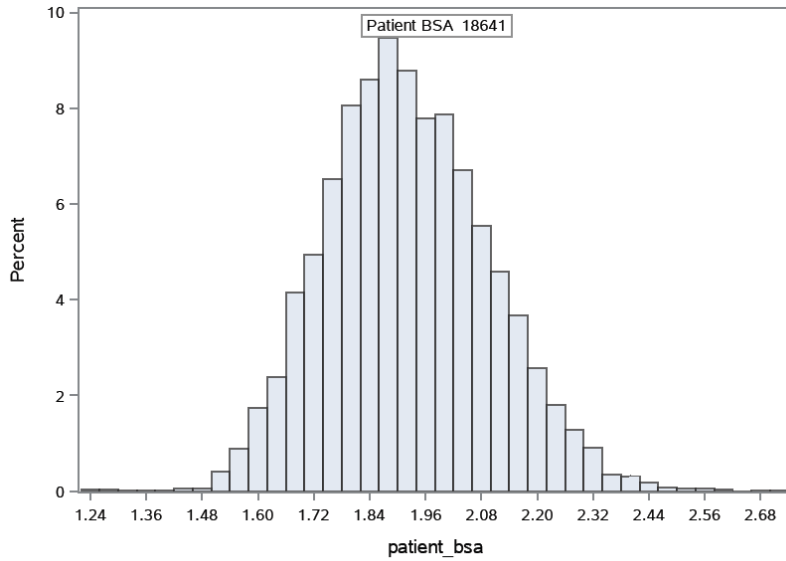
Quantiles (Definition 5)	
Level	Quantile
100% Max	2.31804
99%	2.03458
95%	1.92866
90%	1.87429
75% Q3	1.76302
50% Median	1.63632
25% Q1	1.53425
10%	1.45877
5%	1.40878
1%	1.32634
0% Min	1.03366

Figure 14: BSA Histogram of 157-165 cm Patients



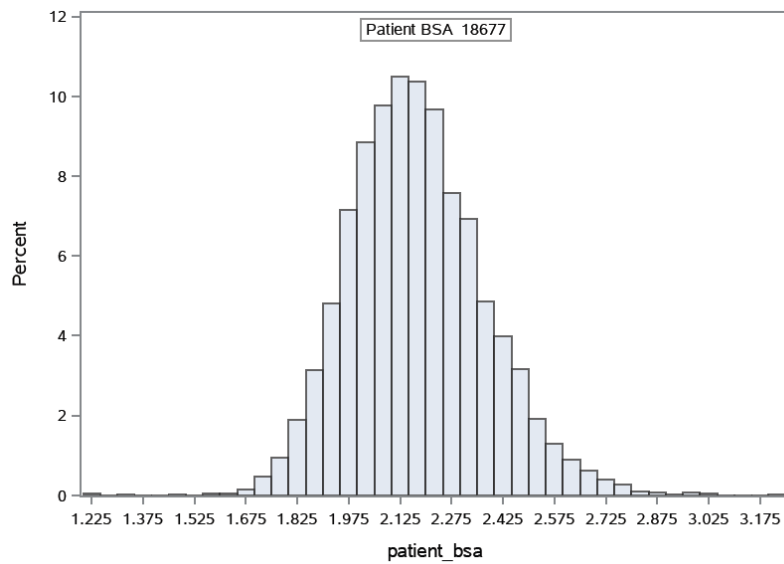
Quantiles (Definition 5)	
Level	Quantile
100% Max	2.57888
99%	2.20805
95%	2.05249
90%	1.98475
75% Q3	1.86796
50% Median	1.74776
25% Q1	1.63664
10%	1.55089
5%	1.49967
1%	1.41770
0% Min	1.16642

Figure 15: BSA Histogram of 166-175 cm Patients



Quantiles (Definition 5)	
Level	Quantile
100% Max	2.72365
99%	2.34734
95%	2.22297
90%	2.15373
75% Q3	2.03878
50% Median	1.91099
25% Q1	1.79946
10%	1.70303
5%	1.64907
1%	1.55777
0% Min	1.25442

Figure 16: BSA Histogram of ≥ 176 cm Patients



Quantiles (Definition 5)	
Level	Quantile
100% Max	3.24683
99%	2.69605
95%	2.51241
90%	2.43060
75% Q3	2.29516
50% Median	2.16134
25% Q1	2.03710
10%	1.93774
5%	1.87478
1%	1.76693
0% Min	1.22324

References

Rockafellar R, Wets RB (1997) *Variational Analysis. Grundlehren der Mathematischen Wissenschaften 317*, Springer.